Research Square

Preprints are preliminary reports that have not undergone peer review.
They should not be considered conclusive, used to inform clinical practice,
or referenced by the media as validated information.

Electricity-Secure Sustainable Closed-Loop Supply Chain Design at the Production-Land-Energy Nexus: A Data-Driven Co-Optimization Framework for the Steel Industry

Milad Askary
Iran University of Science and Technology
Mohammad Reza Mohammad Aliha
Mrm_aliha@iust.ac.ir

Iran University of Science and Technology
Ahmad Makui
Iran University of Science and Technology
Mir Saman Pishvaee
Iran University of Science and Technology

Article

Keywords: Electricity-Secure, On-Site Power Generation, Data-Driven Robust Optimization, Sustainability, Industrial Land Sharing, Closed-Loop Supply Chain

Posted Date: November 13th, 2026

DOI: https://doi.org/10.21203/rs.3.rs-11105562/v1

License: This work is licensed under a Creative Commons Attribution 4.0 International License.
Read Full License

Additional Declarations: No competing interests reported.

Electricity-Secure Sustainable Closed-Loop Supply Chain Design at the Production-Land-Energy Nexus: A Data-Driven Co-Optimization Framework for the Steel Industry

Milad Askary[a], Mohammad Reza Mohammad Aliha[a,b], Ahmad Makui[a], Mir Saman Pishvaee[a]

[a] School of Industrial Engineering, Iran University of Science and Technology, Tehran, Iran

Milad Askary; Email: m_askary@ind.iust.ac.ir; ORCID: 0009-0005-5088-1920

[b] Corresponding author, Mohammad Reza Mohammad Aliha; Email: Mrm_aliha@iust.ac.ir; ORCID: 0000-0001-9451-0949

Ahmad Makui; Email: amakui@iust.ac.ir; ORCID: 0000-0001-6249-530X

Mir Saman Pishvaee; Email: pishvaee@iust.ac.ir; ORCID: 0000-0001-6389-6308

Abstract

Energy shortages, resource scarcity, and limited industrial land can infeasible the attractive steelmaking locations. This study develops an integrated robust optimization framework for a sustainable closed-loop DRI-EAF steel supply chain in which facility location, production-line selection, scrap recovery, wastewater reuse, on-site electricity generation, and industrial-land allocation are co-planned. The central modeling contribution is the endogenous competition for a common, finite land resource between steel production, photovoltaic systems, and diesel-fueled CHP units of different capacities. This coupling allows electricity-constrained candidate locations to remain feasible when the economic and operational value of the site justifies appropriately sized on-site generation. A data driven approach is used to model polynomial regression based on historical temperature, solar-irradiance, and energy-consumption data to estimate location- and period-specific electricity conditions, natural-gas availability, and solar-generation potential; bounded uncertainty is then handled through robust optimization. The multi-objective MILP model proposed to minimize total system cost and CO_2 emissions while maximizing surplus on-site electricity exported to the grid. In the case study, the selected design generates approximately 1.29E+10 kWh of on-site electricity annually, including 6.94E+9 kWh from solar PV, and exports 5.34E+9 kWh to the grid. The associated circular-resource strategy avoids approximately 6.10E+6 t of iron-ore extraction, mitigates approximately 2.80E+9 kg of CO_2 emissions, reuses approximately 2.15E+8 m of wastewater, and creates 7,415 jobs. The results show that industrial land is an active coupling resource between production expansion and energy security, rather than a passive siting parameter, and that coordinated energy-land-production planning can preserve technically constrained but strategically attractive steelmaking locations.

Keywords: Electricity-Secure; On-Site Power Generation; Data-Driven Robust Optimization; Sustainability; Industrial Land Sharing; Closed-Loop Supply Chain

1. Introduction

Steel is a strategic material for infrastructure, transportation, machinery, and industrial development (see Fig. 1). Its production, however, is intrinsically resource- and energy-intensive and therefore depends on reliable access to electricity, natural gas, water, and raw materials. These dependencies are particularly important for the direct-reduction-electric-arc-furnace (DRI-EAF) route, in which iron ore is reduced to sponge iron using natural gas and subsequently melted with steel scrap in an electric arc furnace. Depending on plant configuration, producing one ton of crude steel typically requires approximately 400-500 kWh of

electricity, 1.6-3.3 m of net water, and 250-300 Nm of natural gas (World Steel Association, 2025; Fan & Friedmann, 2021; Shahabuddin et al., 2024). Consequently, expansion decisions that appear economically attractive from a conventional facility-location perspective may become technically infeasible when local electricity, gas, water, or land resources are insufficient. Seasonal meteorological conditions further complicate this planning problem because electricity and natural-gas availability vary across locations and months as regional heating and cooling loads change (Staffell et al., 2023).

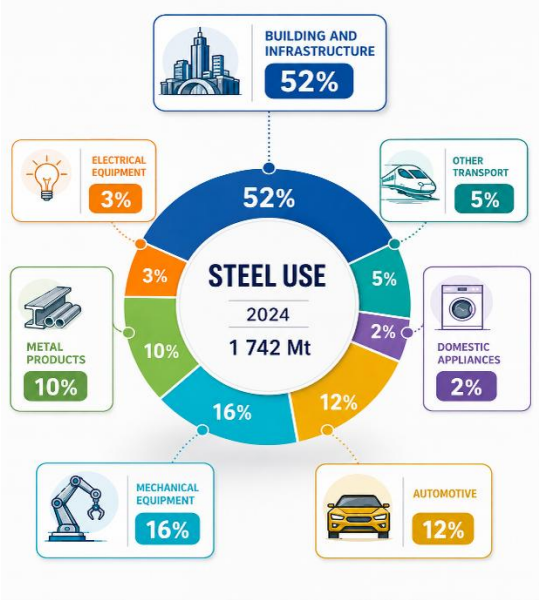


Fig.1 Different use of crude steel in human life (www.worldsteel.org)

Steel-capacity expansion must therefore address energy security, resource efficiency, and industrial decarbonization simultaneously (Harpprecht et al., 2025). Although the DRI-EAF route generally produces less CO_2 than conventional BF-BOF steelmaking, substantial emissions remain associated with natural-gas-based direct reduction, electricity-intensive melting, transportation, and auxiliary energy generation. At the same time, declining ore grades and constraints on primary-resource extraction increase the strategic value of scrap recovery and circular material use (Watari et al., 2025). These considerations connect decisions that are often planned separately: facility location, production capacity, raw-material sourcing, scrap recovery, water reuse, energy procurement, on-site generation, and industrial-land allocation. A closed-loop supply-chain perspective provides an appropriate structure for coordinating these decisions because it integrates forward material flows with reverse flows and resource recovery within a single network-design problem (Amin & Baki, 2017). The planning challenge becomes more difficult when demand, resource availability, energy conditions, and material quality are uncertain, since a nominally optimal network may not remain feasible under adverse realizations (Zokaee et al., 2017).

Accordingly, this study considers the expansion of semi-finished steel production through new DRI-EAF facilities selected from candidate locations with heterogeneous access to electricity, natural gas, water, raw materials, markets, transportation infrastructure, solar resources, and vacant industrial land. The distinguishing decision problem is that steelmaking lines and on-site generation technologies compete for the same finite land resource. Allocating additional land to production increases manufacturing capacity, whereas allocating land to photovoltaic or CHP facilities increases local electricity availability and can restore the feasibility of an energy-constrained site. This endogenous land-energy-production coupling is

embedded in a closed-loop network that also recovers steel scrap and reuses wastewater. Historical meteorological and energy data are used to estimate location- and month-specific energy conditions, while robust optimization protects strategic decisions against bounded parameter uncertainty. The resulting tri-objective MILP therefore evaluates candidate locations only after jointly accounting for production value, resource availability, circular material flows, on-site generation opportunities, land scarcity, cost, CO_2 emissions, and employment requirements.

- The first contribution is a land-constrained co-planning formulation in which steel-production lines and on-site electricity-generation technologies compete endogenously for the same finite industrial land.
- Second, on-site generation is modeled as a feasibility-restoration mechanism: an electricity-deficient but otherwise attractive location can remain selectable when its deficit can be compensated by an economically and environmentally acceptable combination of solar PV and CHP capacity.
- Third, surplus on-site electricity can be exported to the grid, linking industrial self-generation decisions with the regional electricity balance rather than treating energy only as an exogenous input to production.
- Fourth, regression-based estimates derived from historical meteorological and energy data are integrated with robust optimization to represent location- and month-specific electricity, natural-gas, and solar-generation conditions without claiming that the robust uncertainty set itself is learned from data.
- The integrated framework additionally captures scrap recovery, wastewater reuse, CO_2 emissions, and employment requirements so that the consequences of the land-energy-production decisions can be evaluated across the economic, environmental, and social dimensions of sustainability.
- Three conflicting objectives are considered: minimizing total system cost, maximizing surplus on-site electricity supplied to the grid, and minimizing total CO_2 emissions.
- The model is solved using an augmented epsilon-constraint procedure to generate nondominated alternatives for the economic-energy-environmental trade-off.
- A real-world Iranian steel-industry case demonstrates the operational implications of the proposed co-planning framework under heterogeneous regional resource conditions.

The remainder of this study is organized as follows. Section 2 reviews the relevant literature and establishes the research gap. Section 3 defines the decision problem and assumptions. Section 4 presents the mathematical formulation, regression-informed energy estimation, robust counterpart, and raw-material cost structure. Section 5 reports the case study and computational results. Section 6 interprets the integrated performance and managerial implications. Section 7 analyzes Pareto trade-offs, verification, and validation, and Section 8 concludes the study.

2. Literature Review

Steel supply-chain research has progressed from conventional cost-oriented planning toward integrated network models that incorporate sustainability, circularity, and resource constraints. Pinto and Diemer (2020) reviewed steel-supply-chain integration and circularity, while Almeida et al. (2022) developed optimization-based sales and operations planning for integrated steel production. More recent studies have

emphasized environmental performance and decarbonization because steelmaking remains highly energy intensive and carbon intensive (Fan and Friedmann, 2021; Na et al., 2024; Harpprecht et al., 2025). Supply-chain optimization has consequently been used to coordinate economic and environmental decisions, including CO_2-related costs, renewable-energy substitution, production-pathway redesign, and low-carbon capacity planning (Zhou et al., 2023; Wu et al., 2025; Shen et al., 2025). Sustainable supply-chain network design further extends this perspective by incorporating social performance together with economic and environmental criteria (Tehrani and Gupta, 2021; Becerra et al., 2024; Afroozi et al., 2025).

Circularity is particularly relevant to steel because recovered scrap can substitute for primary iron-bearing material and can be reintegrated into EAF production. Closed-loop supply-chain models have therefore examined collection, recycling, and reverse-logistics decisions across multiple industrial sectors (Al-Refaie et al., 2021; Shahedi et al., 2022; Baghizadeh et al., 2021). In the steel context, Nikian et al. (2023) incorporated scrap recovery within a sustainable and resilient network. The broader circular-economy literature similarly demonstrates that material recovery can reduce primary-resource dependence while creating additional network-design decisions concerning collection, storage, processing, and reintegration. For the present problem, scrap recovery is not treated as an isolated environmental activity; it is coupled with production, material balance, transportation, energy consumption, and resource requirements within the same network.

Uncertainty is another established concern in strategic supply-chain design. Stochastic programming is appropriate when probability distributions can be estimated reliably, whereas robust optimization is useful when uncertain coefficients are more defensibly represented by bounded sets and decisions must remain feasible under adverse realizations (Zokaee et al., 2017; Wang et al., 2024). Robust and related uncertainty-aware formulations have been applied to blood, vaccine, agri-food, dairy, automotive, and steel planning problems (Razavi et al., 2021; Gilani and Sahebi, 2022; Gholian-Jouybari et al., 2023; Petrova et al., 2023; Lotfi et al., 2025; Wang et al., 2024). In the present study, robust optimization is used specifically to protect strategic network and resource-allocation decisions against bounded deviations in uncertain input parameters; it is therefore conceptually separated from the regression module used to estimate seasonal energy conditions.

Data-driven methods are increasingly used to characterize energy demand and resource availability when direct analytical relationships are difficult to specify. Historical data, regression, and machine-learning methods can reveal dependencies between meteorological conditions and electricity or natural-gas consumption and can thereby improve the parameterization of energy-planning models (Amasyali et al., 2018; Zhu et al., 2022; Jin et al., 2023; Sievers & Blank, 2023). Importantly, the term data-driven robust optimization is also used in the literature for approaches that construct uncertainty sets directly from historical data. A particularly close steel-supply-chain study by Khalili-Fard et al. (2024) develops such a data-driven robust framework using support-vector clustering to design a sustainable circular steel network. The present work differs methodologically: historical meteorological-energy data are used to estimate location- and period-specific energy conditions, whereas bounded robust optimization is then applied as a distinct protection layer for uncertain parameters.

The energy dimension of supply-chain design has also expanded beyond exogenous energy procurement toward renewable integration, self-generation, grid interaction, and coupled resource planning. Renewable-

fuel and bioenergy studies jointly evaluate cost, emissions, land, water, social effects, and feedstock availability (Farajiamiri et al., 2023; Rani et al., 2025; Alharairi et al., 2026), while renewable-energy supply-chain models increasingly consider circularity, reliability, and reverse logistics (Giri & Roy, 2024; Salehi Moghadam et al., 2024). For steel, Wu et al. (2025) address multi-stage low-carbon capacity planning with wind-gas-hydrogen energy, and Fuhrlaender et al. (2025) analyze integrated operating concepts that connect steel transformation with power-system stability. These studies demonstrate the importance of energy-production coordination, but they do not resolve the specific network-design question considered here: how finite industrial land should be allocated endogenously between steel-production capacity and alternative on-site generation technologies when local energy availability itself affects candidate-site feasibility.

Meteorological variability provides the operational link between regional energy conditions and industrial planning. Electricity demand is seasonally sensitive and is influenced by temperature, particularly through heating and cooling loads (Emodi et al., 2018; Garrido-Perez et al., 2021; Staffell et al., 2023). Natural-gas consumption likewise responds strongly to temperature during heating periods (Min et al., 2022; Bugajski et al., 2024), while solar generation depends on irradiance and temperature-sensitive photovoltaic performance (Shaker et al., 2024; Varne et al., 2024). These relationships motivate location- and month-specific energy parameters rather than fixed annual capacities. Tables 1 and 2 synthesize the traditional supply-chain attributes and the emerging energy-related attributes covered in the reviewed literature; the research gap is then stated in terms of the intersection of land, energy, production, and closed-loop network decisions rather than the isolated presence of individual sustainability features.

2.1 Research gap

The literature reveals a clear integration gap rather than a lack of research on any single component. Sustainable and closed-loop steel-supply-chain models already address cost, emissions, social criteria, recycling, and uncertainty, and recent data-driven robust studies have further strengthened uncertainty representation in steel networks. Energy-system studies also examine renewable integration, resource balancing, and climate-sensitive demand. What remains insufficiently addressed is the strategic co-planning problem in which production capacity and on-site electricity generation compete for the same finite industrial land, while location- and period-specific energy conditions determine whether a candidate steelmaking site remains feasible. Existing studies generally treat industrial land as a fixed siting attribute, energy availability as an exogenous capacity, or renewable investment as a separate energy decision. This study closes the intersection gap by embedding land allocation, steel-production-line selection, solar-PV and CHP sizing, grid export, closed-loop scrap recovery, and regression-informed seasonal energy availability within one robust tri-objective network-design model. The novelty therefore lies primarily in the endogenous land-energy-production coupling and its effect on facility feasibility; circularity, water reuse, emissions, and employment are integrated to quantify the broader sustainability consequences of those strategic decisions.

Table. 1 Energy-oriented literature review

Reference	Land Sharing	Data Driven	Grid Injection	Renewable Energy	On Site Generation	Recycle	Meteorological	Energy Balancing	Case Study
Arslan & Kara, 2026				√	Solar				
Askary et al., 2026		√				√	√	√	Petroleum
Yazdi et al.,2026			√	√	Solar Wind				Power Plant
Saeed et al., 2026						√			Electronic
Lotfi et al., 2025				√	Solar	√			Automotive
Panjehpour & Zarrinpoor, 2025				√	Biofuel				Agricultural
Rani et al., 2025				√	Biofuel	√			
Valizadeh et al., 2025						√			Pipe
Wu et al., 2025				√	Solar				Steel
Hosseini et al., 2025						√			Food
Darabad et al., 2025						√			Chemical
Becerra et al., 2024						√			Mining
Khot et al., 2024						√			Pipe
Askary et al., 2024									Steel
Taherifar et al., 2024						√			Home Appliance
Wang et al., 2024									Steel
Giri & Roy, 2024			√	√	Biofuel Solar	√			Waste
Nikian et al., 2023						√			Steel
Zhou et al., 2023									Electronic
Mohammadi & Nikzad, 2023						√			
Mohammadi et al., 2023									Food
Fasihi et al., 2023						√			Food
Shahedi et al., 2022						√			Automotive
Gilani & Sahebi, 2022		√							Health
Baghizadeh et al., 2021						√			Tire
Tehrani & Gupta, 2021						√			Tire
Al-Refaie et al., 2021						√			Air Conditioning
Pinto & Diemer, 2020									Steel
This Work	√	√	√	√	Solar CHP	√	√	√	Steel

Table. 2 Supply chain- oriented literature review

Reference	Model	Objectives	Economic	Pollution	Social	Uncertainty	Period	Product
Arslan & Kara, 2026	MILP	**Min**. Cost; **Min**. Environmental Effect **Max**. Renewable Energy; **Min**. Water	√	CO_2	√	ST	S	M
Askary et al., 2026	MILP	**Min**. Cost; **Min**. Environmental Effect	√	CO_2		ST; D	M	M
Yazdi et al.,2026	MIQP	**Min**. Cost; **Min**. Environmental Effect	√	CO_2			S	M
Saeed et al., 2026	MILP	**Max**. Profit; **Min**. Environmental Effect **Max**. Job; **Min**. Risk	√	CO_2	√	ST	M	S
Lotfi et al., 2025	MINLP	**Min**. Sustainability Cost	√	CO_2	√	ST	M	M
Panjehpour & Zarrinpoor, 2025	MINLP	**Max**. Crop Collection **Min**. Lost Value; **Max**. Profit	√	CO_2		F	M	M
Rani et al., 2025	MILP	**Min**. Cost; **Max**. Job **Min**. Environmental Effect	√		√		M	S
Valizadeh et al., 2025	MILP	**Min**. Sustainable Risk; **Min**. Cost	√		√	ST	S	M
Wu et al., 2025	MILP	**Min**. Cost; **Max**. Efficiency **Max**. Peak Regulation	√		√		M	M
Hosseini et al., 2025	MILP	**Min**. Cost; **Max**. Job **Min**. Environmental Effect	√	CO_2	√	ST	M	M
Darabad et al., 2025	MILP	**Min**. Cost; **Min**. Time	√			F	M	M
Becerra et al., 2024	MINLP	**Min**. Cost; **Min**. Environmental Effect **Min**. Accidents; **Max**. Job	√	CO_2	√		M	S
Khot et al., 2024	MINLP	**Min**. Cost; **Min**. Environmental Effect **Min**. Social Responsibility	√	CO_2	√	F	M	M
Askary et al., 2024	MINLP	**Min**. Cost; **Max**. Location Score **Max**. Efficiency	√		√	ST	S	M
Taherifar et al., 2024	MILP	**Min**. Cost; **Min**. Environmental Effect **Min**. Social Responsibility	√	CO_2	√	ST	S	M
Wang et al., 2024	MILP	**Min**. Cost	√			ST; D	M	M
Giri & Roy, 2024	MILP	**Min**. Cost; **Max**. Job **Min**. Environmental Effect	√	CO_2	√		M	M
Nikian et al., 2023	MILP	**Max**. Profit; **Min**. Environmental Effect **Min**. Transmission Virus	√	GHG	√	ST	S	M
Zhou et al., 2023	MILP	**Min**. Cost	√	CO_2			S	S
Mohammadi & Nikzad, 2023	MILP	**Min**. Cost; **Min**. Environmental Effect **Max**. Job; **Min**. Infection Risk	√	CO_2	√	ST	M	M
Mohammadi et al., 2023	MINLP	**Max**. Profit; Max. Job; **Min**. Environmental Effect	√	CO_2	√		S	M
Fasihi et al., 2023	MILP	**Min**. Cost; Min. Environmental Effect **Max**. Reaction Time	√	CO_2	√	ST	M	M
Shahedi et al., 2022	MILP	**Max**. Profit; **Max**. Job **Min**. Environmental Effect	√	CO_2	√	ST	M	S
Gilani & Sahebi, 2022	MILP	**Min**. Cost; **Max**. Job **Min**. Environmental Effect	√	GHG	√	D	M	M
Baghizadeh et al., 2021	MINLP	**Min**. Cost; **Min**. Environmental Effect **Max**. Job **Max**. Resiliency	√	CO_2	√	F	S	S
Tehrani & Gupta, 2021	MILP	**Max**. Profit; **Max**. Job **Min**. Environmental Effect	√	CO_2	√	ST; F	M	M
Al-Refaie et al., 2021	MILP	**Max**. Profit	√	GHG	√	ST	M	M
Pinto & Diemer, 2020	MILP	**Max**. Profit	√			ST	M	M
This Work	MILP	**Min**. Cost; **Min**. Environmental Effect **Max**. power Injection to grid	√	CO_2	√	D	M	M

M: Multi; **S**: Single

ST: Stochastic; **F**: Fuzzy; **D**: Deep

MILP: Mixed Integer Linear Programming; **MINLP**: Mixed Integer Nonlinear Programming; **MIQP**: Mixed Integer Quadratic Programming

3. Problem Statement

This study develops an integrated sustainable closed-loop steel supply-chain network for satisfying unmet demand for semi-finished steel products under heterogeneous regional resource constraints. As illustrated in Fig. 2, the network comprises iron-ore suppliers, steel-scrap collection centers, candidate .steelmaking facilities, downstream customers, energy inputs, and water-management components Forward flows include iron ore, recovered scrap, and finished steel products, whereas reverse flows recover post-use or process-generated scrap and support wastewater reuse. The network-design problem jointly determines facility opening, production-line installation, material flows, inventories, resource .consumption, on-site generation, and industrial-land allocation

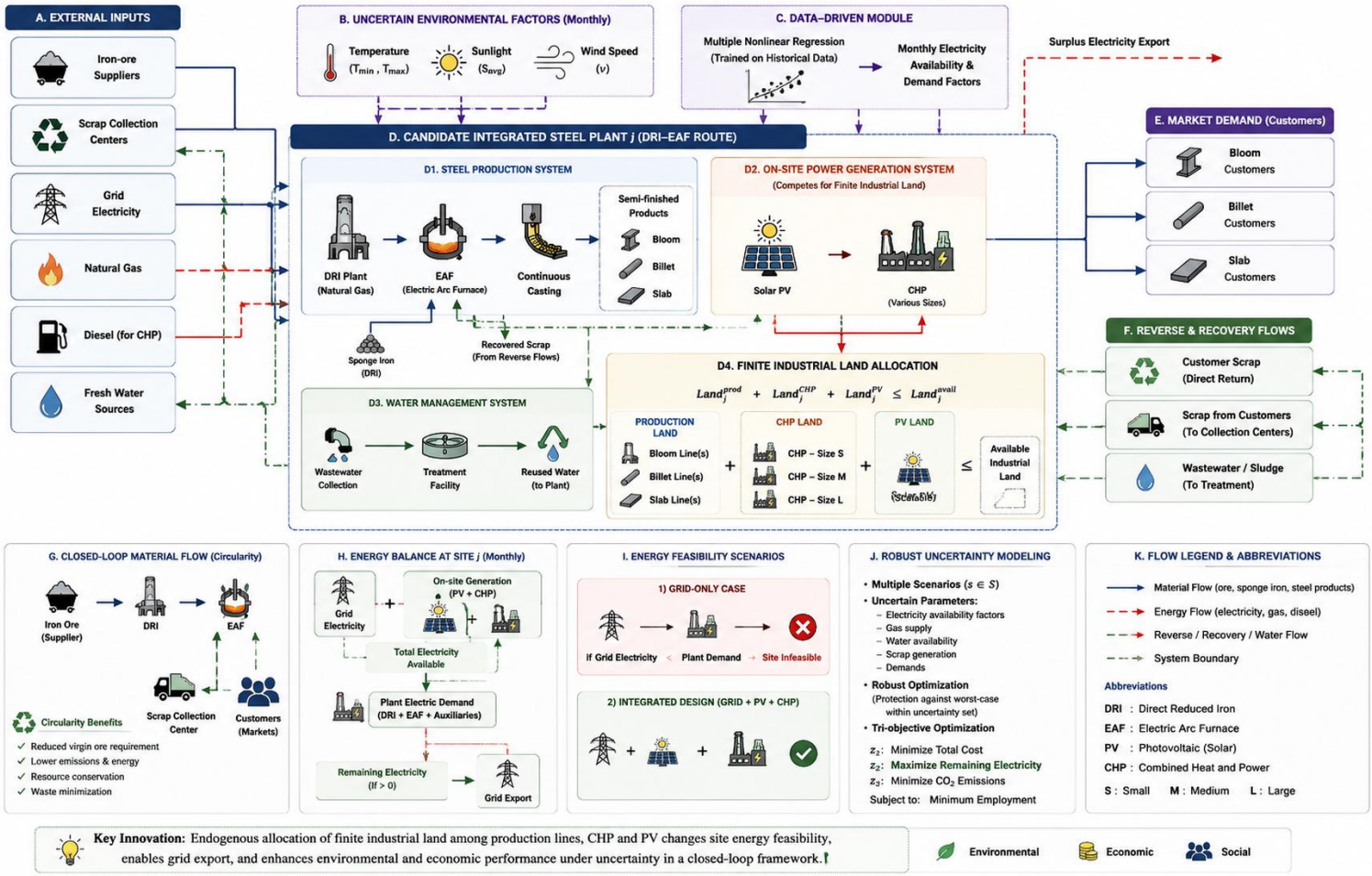


Fig.2 Conceptual model of proposed model

Each candidate steel facility contains the principal stages of the DRI-EAF route: direct reduction, electric-arc-furnace processing, and continuous casting. Iron ore is converted to sponge iron using natural gas, after which sponge iron and recovered steel scrap are charged to the EAF. Molten steel is then cast as bloom, billet, or slab according to the installed production lines. Because scrap enters the EAF material balance, reverse-logistics decisions directly affect virgin-ore requirements, transportation activity, energy consumption, and production-resource use rather than operating as a separate recycling subsystem.

The central planning difficulty is the simultaneous scarcity of electricity and industrial land. Candidate sites differ in grid electricity, natural gas, water, diesel supply, solar conditions, market access, transportation distances, and vacant land. Grid limitations can make a location technically infeasible even when it is favorable in terms of demand access or logistics. The model therefore permits two on-site electricity-generation alternatives: photovoltaic systems and CHP units available in small, medium, and large capacity classes. Each technology is characterized by electrical capacity, land requirement, investment and operating costs, resource consumption, employment contribution, and CO_2 emissions where applicable. For CHP, only the electrical subsystem is represented within the model boundary; thermal output is neither used nor credited economically or environmentally. Solar-generation capacity is determined by the land allocated to photovoltaic systems together with period-specific irradiance and temperature conditions. Local on-site generation first contributes to the electricity required by steel production; any remaining eligible on-site electricity is represented as surplus that can be exported to the external grid. Energy availability is not assumed constantly across the planning horizon. Historical temperature, solar-radiation, and electricity-consumption data are used to estimate location-specific monthly energy conditions, and temperature-dependent functions are used for natural-gas availability. This regression-informed parameterization captures seasonal meteorological effects without treating short-term weather variation as a long-term climate-change scenario. Because meteorological, resource, and material parameters remain subject to estimation error and adverse variation, selected uncertain coefficients are represented by bounded intervals and handled through robust optimization. The robust layer is intended to protect strategic facility, land-allocation, production-capacity, and energy-investment decisions against unfavorable parameter realizations when reliable probability distributions are not available.

The distinctive coupling arises because steel production lines and on-site generation facilities compete for the same finite land. More land assigned to manufacturing supports production capacity, whereas land assigned to PV or CHP increases electricity availability and can preserve the feasibility of an electricity-constrained location. Consequently, land is modeled as an active shared resource linking industrial expansion and energy security (Fig. 3).

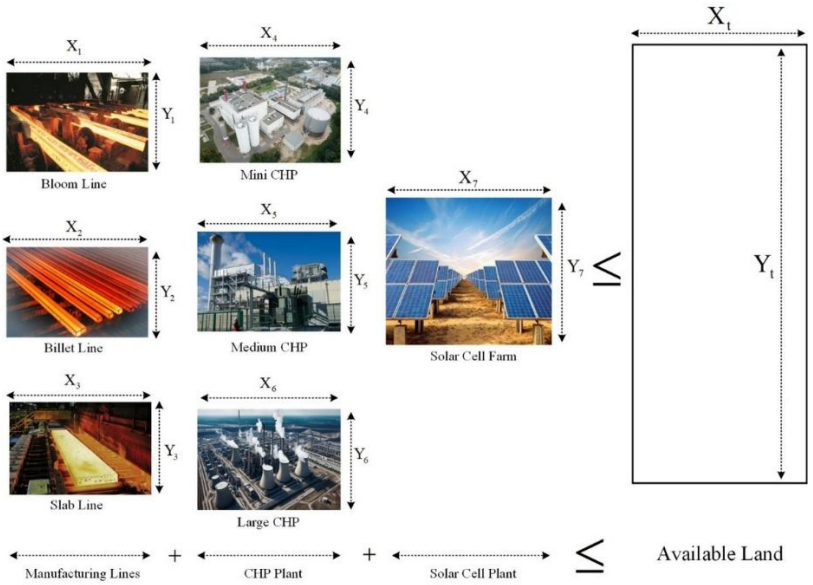


Fig. 3 Land use optimization address to on-site power generation

Economic, environmental, energy, and social consequences are evaluated simultaneously through the multi-objective formulation.

1. Minimizes total system costs
2. Maximizes surplus on-site electricity exported to the grid
3. Minimizes co_2 emissions arising from steel production, transportation, and on-site generation

Social sustainability is represented by a minimum employment requirement associated with selected steel-production lines and on-site energy facilities. The exact multi-objective procedure generates nondominated alternatives across cost, grid-support, and CO_2 objectives. The principal methodological contribution is therefore not the independent inclusion of multiple sustainability features, but their coordination around a shared land-energy-production decision: each candidate site is evaluated only after its production potential, seasonal resource constraints, land availability, self-generation options, circular material flows, environmental impacts, and employment contribution are considered jointly.

3.1. Model assumptions

Before presenting the mathematical model, the following assumptions define the system boundary and decision logic.

- The planning horizon consists of monthly periods with constant parameters within each period.
- Electricity cannot be stored; it must be consumed or exported to the grid in the same period.
- Product demand must be fully satisfied without shortages, lost sales, or back orders.
- A steel facility can open only if at least one production line is installed.
- On-site solar and CHP power facilities can be installed only at operating steel sites.
- Grid electricity, natural gas, water, and fuel availability vary by location and period.
- Total land use for production and power-generation facilities cannot exceed the available land at each location.

- Technology capacities, land requirements, investment costs, and operating characteristics are known.
- The proportions of sponge iron and scrap in the EAF are determined by material balance and production requirements.
- Generated steel scrap may be collected, stored, and returned to the EAF within network capacity limits.
- Materials and products are transported by road, with costs and emissions proportional to quantity and distance.
- Solar generation depends on the allocated land area, solar irradiance, and ambient temperature.
- Uncertain meteorological, resource, and material parameters are represented by bounded intervals and handled through robust optimization.
- Strategic investment decisions remain fixed, while operational decisions may vary over periods.
- CHP units are represented through their electrical output, fuel consumption, water requirement, operating cost, land use, employment contribution, and CO_2 emissions; thermal-energy recovery, storage, utilization, and any associated credit are outside the system boundary.
- Accordingly, the term CHP in this study identifies the physical on-site generation technology, while the optimization accounts only for the electrical service relevant to the investigated steel-network planning problem.

4. Mathematical model

Based on the preceding problem definition, a robust mixed-integer linear programming model is formulated to co-plan closed-loop material flows, steel-production capacity, industrial land, and on-site electricity generation under bound uncertainty. The sets, parameters, and decision variables are defined below; the mathematical expressions themselves are retained as the formal specification of the model.

Sets	
I	Index for iron ore suppliers
J	Index for candidate location
K	Index for steel scrap center
L	Index for consumers (downstream manufactures)
PC	Index for CHP plant types
T	Index for period
U	Index for product types

Parameters	
$\mathrm{demand}_{l,u}$	Demand for each product u by each consumer l (ton)
$\mathrm{dmf}_{i,j}$	Distance between supplier i and candidate location j (Km)
$\mathrm{dsf}_{k,j}$	Distance between steel scrap center k and candidate location j (Km)
$\mathrm{dfc}_{j,l}$	Distance between candidate location j and consumer l (Km)
$\mathrm{dcs}_{l,k}$	Distance between consumer l and steel scrap center k (Km)
Trc	Unit cost for transportation ($ per ton. kilometer)
Prc_{u}	Fixed cost to developing manufacturing line for product u ($)
fs_{j}	Fixed cost for initial manufacturer structure ($)

$CHPf_{pc}$	Fixed Cost for opening each CHP type pc ($)
Cdsl	Fixed cost for each solar cell ($)
Cxs	Operational cost for manufacturing one ton sponge iron ($ per ton)
Cxp_u	Operational cost for manufacturing one ton product u ($ per ton)
Coch	Operational cost for generating one kwh power by CHP ($ per Kwh)
Czss	Operational cost for generating one kwh by power solar ($ per Kwh)
$Cape_{j,t}$	Average electracy power available in each candidate location j (kwh per month)
$Capg_{j,t}$	Average natural gas available in each candidate location j (m^3 per month)
$Capw_{j,t}$	Average water available in each candidate location j (m^3 per month)
$Rland_u$	Amount of land used to installation each manufacturing line u (m^2)
$Landin_j$	Average land available in each candidate location j (m^2)
$Op_{k,t}$	Average steel scrap recycling result of operational steel scrap center k (ton)
Stsc	Unit cost for steel scrap in second price ($ per ton)
Nstc	Unit cost for steel scrap in first price ($ per ton)
Orc_i	Unit cost for buying iron ore ($ per ton)
Ce	Unite cost for electric power ($ per kwh)
Cgs	Unit cost for natural gas ($ per m^3)
Cgsl	Unite cost for diesel fuel ($ per litter)
Cwt	Unite cost for water ($ per m^3)
Crtw	Unite cost for water treatment ($ per m^3)
Cds	Penalty cost for water disposal ($ per m^3)
Hpr_u	Unit holding cost for product u ($ per ton)
Hss	Unit holding cost for steel scrap ($ per ton)
Hw	Unit holding cost for Water ($ per m^3)
Landc	Unite cost for land use ($ per m^2)
$Rchp_{pc}$	Amount of land used to installation each CHP type pc (m^2)
Rgs	Rate of using natural gas to manufacture a one crude steel (m^3 per ton)
Rgsl	Diesel-fuel consumption rate of CHP (Litter/kWh)
Rep	Rate of using electricity power to manufacture a one crude steel (Kwh per ton)
Rdr	Rate of using electricity power in direct reduction (Kwh per ton)
Rwt	Rate of water to manufacture a one crude steel (m^3 per ton)
Rtw	Rate of water treatment (percentage)
Rchw	Rate of using water to generate a one kwh power electricity (m^3 per kwh)
Rs	Rate of residual steel results of cuttings (percentage)
Rsp	Average rate of sponge iron in EAF (percentage)
Rsc	Average rate of scrap in EAF (percentage)
$Tm_{j,t}$	Average Temperature in each candidate location j at period t (Celsius)
$Calfe_i$	Iron ore grade of supplier i (percentage)
$Ssh_{j,t}$	Average sunlight in each candidate location j at period t (hours)
Dsl	Area of each solar cell (m^2)

Tref	Standard temperature for cell solar (Celsius)
$CHPo_{pc}$	Maximum operational power of CHP type pc
G_{max}	Maximum solar irradiance (W/m²)
Egs	Rate of CO_2 emission pollution to manufacture a one crude steel (kg per ton)
Etr	Rate of CO_2 emission pollution for transportation (kg per ton. kilometer)
Egsl	Rate of CO_2 emission pollution to generate a one kwh electricity power in CHP (kg per kwh)
$Emf_{j,u}$	Rate of employment for each opening manufacturing u in candidate location j (person)
$Emch_{pc}$	Rate of employment for each CHP type pc (person)
Ems	Rate of employment for each kwh electricity power in solar plant (person)
Spj	Social program for creating new job opportunities (person)
Asv	Average salvage must pay to employers ($)
Mb	A big number

Variables	
Class.1 variables are Binary Variables $\in \{0,1\}$	
$Z_{j,u}$	If manufacturing line u open in candidate location j is 1 else is 0.
X_j	If in candidate location j at least one manufacturing line is open 1 else is 0.
$ych_{j,pc}$	If in candidate location j CHP type pc open is 1 else is 0.
ysl_j	If in candidate location j solar power open is 1 else is 0.
Class.2 variables are Positive Variables ≥ 0	
$xmf_{i,j,t}$	Amount of iron ore send from supplier i to manufacturer j at period t
$xfc_{j,u,l,t}$	Amount of product u send from manufacturer j to consumer l at period t
$xsf_{k,j,t}$	Amount of steel scrap send from steel scrap center k to manufacturer j at period t
$xcf_{l,j,t}$	Amount of steel scrap send from consumer l to manufacturer j at period t
$xcs_{l,k,t}$	Amount of steel scrap send from consumer l to steel scrap center k at period t
$Xre_{j,t}$	Amount of electricity power consume in candidate location j at period t
$Zmeth_{j,t}$	Amount natural gas consume in candidate location j at period t
$zw_{j,t}$	Amount water consumption in manufacturer j at period t
$zwt_{j,t}$	Amount water treatments in candidate location j at period t
$zwc_{j,t}$	Amount water consumes in CHP j at period t
$zwd_{j,t}$	Amount water disposal in CHP candidate location j at period t
$Inne_t$	Electricity power status in network at period t without considering Self-Sustained power
$Inns_t$	Electricity power status in network at period t with considering Self-Sustained power
$Slfe_{j,t}$	Self-Sustained power generated in candidate location j at period t
$Rsle_{j,t}$	surplus of Self-Sustained power generated in candidate location j at period t
$Xprs_{j,t}$	Amount of manufacturing sponge iron by manufacturer j at period t
$Xprp_{j,u,t}$	Amount of manufacturing product u by manufacturer j at period t

$Zsch_{j,t}$	Amount of electricity power generated by CHP in candidate location j at period t
$Zss_{j,t}$	Amount of electricity power generated by solar cell in candidate location j at period t
$Invf_{j,u,t}$	Inventory of product u in manufacturer j at period t
$Invs_{k,t}$	Inventory of scrap in steel scrap center k at period t
$Invw_{j,t}$	Inventory of water in manufacturer j at period t
Lf_{j}	Amount of land use at candidate location j
$Lchp_{j,pc}$	Amount of land use at candidate location j by CHP type pc
Lsl_{j}	Amount of land use by solar cells in candidate location j
$Fco_{j,t}$	Amount of CO_2 pollution by manufacturer j at period t
$CHco_{j,t}$	Amount of CO_2 pollution by CHP type pc at period t
$Trco_{t}$	Amount of CO_2 pollution results of transportations at period t

The model contains three objective functions. The first objective minimizes total system cost, including facility and production-line investment, procurement, production, transportation, reverse logistics, energy and water use, land allocation, on-site generation, employment-related costs, and inventory holding, as defined in Eq. (1).

$$Z_1 = ZTC + ZTM + ZTF + ZEM + ZOM + ZTL + ZTW + ZTFU + ZTH + ZTCH + ZSLP \tag{1}$$

The transportation-cost component is defined in Eq. (2) and includes material shipments to manufacturers, recovered scrap flows, product deliveries to customers, direct reverse flows, and customer-to-collection-center scrap movements.

Total Transportation Cost = shipments of materials to manufacturers + recovered scrap from scrap collection centers to manufacturers + products from manufacturers to customers + returns from customers to manufacturers + steel scrap from customers to scrap collection centers

$$\begin{aligned} ZTC = &\sum_i \sum_j \sum_t Trc.dmf_{i,j}.xmf_{i,j,t} + \sum_k \sum_j \sum_t Trc.dsf_{k,j}.xsf_{k,j,t} + \sum_j \sum_u \sum_l \sum_t Trc.dfc_{j,l}.xfc_{j,u,l,t} \\ &+ \sum_l \sum_j \sum_t Trc.dcf_{l,j,t}.xcf_{l,j,t} + \sum_l \sum_k \sum_t Trc.dcs_{l,k}.xcs_{l,k,t} \end{aligned} \tag{2}$$

The raw-material cost component in Eq. (3) includes iron-ore procurement, scrap purchased from collection centers, and scrap acquired through reverse-logistics flows.

Total Raw Material Cost = iron ore purchasing costs + steel scrap purchasing costs from scrap collection centers + reverse-logistics scrap acquisition costs

$$ZTM = \left(\sum_i \sum_j \sum_t Orc_i.xmf_{i,j,t} + \sum_k \sum_j \sum_t Stsc.xsf_{k,j,t} + Nstc.\left(\sum_j \sum_u \sum_l \sum_t xfc_{j,u,l,t} + \sum_l \sum_k \sum_t xcs_{l,k,t} \right) \right) \tag{3}$$

The fixed-cost component in Eq. (4) includes the initial facility structure and installed manufacturing lines.

Total Fixed Cost = Initial structure cost + manufacturing lines cost

$$\sum_j X_j.fs_j + \sum_j \sum_u Z_{j,u}.Prc_u \tag{4}$$

The employment-related cost component is defined in Eq. (5).

Total Employing Cost = employing cost in manufacturers + employing cost in CHP plants + employing cost in solar plants

$$ZEM=\left(\sum_{j}\sum_{u} Z_{j,u}.Emf_{j,u}+\sum_{j}\sum_{pc} ych_{j,pc}.Emch_{pc}+\sum_{j}\sum_{t} zss_{j,t}.Ems\right).Asv \quad (5)$$

The manufacturing operating-cost component in Eq. (6) includes sponge-iron production and crude-steel production costs.

Total Manufacturer Operational Cost = sponge iron manufacturing cost + crude steel manufacturing cost

$$ZOM=\sum_{j}\sum_{t} Cxs.xprs_{j,t}+\sum_{j}\sum_{u}\sum_{t} Cxp.xprp_{j,u,t} \quad (6)$$

The land-use cost component in Eq. (7) accounts for land assigned to manufacturing, solar-PV facilities, and CHP units.

Total Land Use Cost = land cost for manufacturing + land cost for solare plant + land cost for CHP plant

$$ZTL=\left(\sum_{j} Lf_{j}+\sum_{j} Lsl_{j}+\sum_{j}\sum_{pc} Lchp_{j,pc}\right).Landc \quad (7)$$

The water-cost component in Eq. (8) includes manufacturing water, water treatment, disposal, and CHP water use.

Total Water Cost = water cost for manufacturing + water treatment cost + water disposal cost + water cost for CHP

$$ZTW=\sum_{j}\sum_{t} Cwt.zw_{j,t}+\sum_{j}\sum_{t} Rwt.Crtw.zw_{j,t}+\sum_{j}\sum_{t}(1\text{-}Rtw).Cds.zw_{j,t}+\sum_{j}\sum_{pc}\sum_{t} Rwchp_{pc}.Cwt.zsch_{j,t} \quad (8)$$

The fuel-cost component in Eq. (9) includes natural gas used for DRI production and diesel fuel consumed by CHP-based electricity generation.

Total Fuel Cost = natural-gas cost for DRI production + diesel-fuel cost for CHP-based electricity generation

$$ZTFU=\sum_{j}\sum_{t} Rgs.Cgs.xprs_{j,t}+\sum_{j}\sum_{t} Rgsl.Cgsl.zsch_{j,t} \quad (9)$$

The inventory-cost component in Eq. (10) includes holding costs for products, steel scrap, and water.

Total Inventory Cost = holding cost for products + holding cost for steel scrap + holding cost for water

$$ZTH=\sum_{j}\sum_{u}\sum_{t} Hpr_{u}.Invf_{j,u,t}+\sum_{k}\sum_{t} Hss.Invs_{k,t}+\sum_{j}\sum_{t} Hw.Invw_{j,t} \quad (10)$$

The CHP cost component in Eq. (11) includes fixed and operating costs.

Total CHP Cost = fixed cost + operational cost

$$ZTCH=\sum_{j}\sum_{pc} CHPf_{pc}.ych_{j,pc}+\sum_{j}\sum_{t} Coch.zsch_{j,t} \quad (11)$$

The solar-PV cost component in Eq. (12) includes fixed and operating costs.

Total Solar Plant = fixed cost + operational cost

$$ZTSLP=\sum_{j}\left(\frac{Cdsl.Lsl_{j}}{Dsl}\right)+\sum_{j}\sum_{t}Czss\ .zss_{j,t} \tag{12}$$

The second objective maximizes the remaining electricity capacity available for export to the grid after accounting for production requirements, grid availability, and on-site generation, as defined in Eq. (13).

$$Z_2 = RSFP \tag{13}$$

The aggregate remaining-electricity measure is defined in Eq. (14).

Remaining Electricity Capacity = sum of the rest power electricity in all location

$$RSFP=\sum_{j}\sum_{t}Rsle_{j,t} \tag{14}$$

Equation (15) defines the location- and period-specific electricity balance underlying the export objective.

Remain Electricity Power = potential capacity of network + on-site power generation + power consumption + monthly fluctuations

$$Rsle_{j,t} = Cape_{j}.X_{j} + Zss_{j,t} + Zsch_{j,t} - Xre_{j,t} - Rpw_{j,t} \tag{15}$$

Manufacturing electricity consumption is defined in Eq. (16) from the requirements of sponge-iron production and EAF steelmaking.

Power Consumption = electricity required for sponge iron production + electricity consumed by the electric arc furnace (EAF)

$$Xre_{j,t} = \sum_{j}\sum_{u}\sum_{t}Xprp_{j,u,t}.Rep + \sum_{j}\sum_{t}Xprs_{j,t}.Rdr \tag{16}$$

The third objective minimizes total CO_2 emissions from steel manufacturing, transportation, and CHP-based on-site generation, as defined in Eq. (17).

Total CO_2 Emission Pollution = manufacturing pollutions + transportation pollutions + CHP plant pollutions

$$Z_3 = ETF + ETTR + ETCH \tag{17}$$

The corresponding emission components are specified in Eqs. (18)-(20).

$$ETF = \sum_{j}\sum_{t}fco_{j,t} \tag{18}$$

$$ETTR = \sum_{t}Trco_{t} \tag{19}$$

$$ETCH = \sum_{j}\sum_{t}CHco_{j,t} \tag{20}$$

The remaining model constraints are given in Eqs. (21)-(59) and enforce the network, material-balance, capacity, land, energy, water, environmental, social, and variable-domain requirements described below.

$$X_{j} \geq \frac{\sum_{u} Z_{j,u}}{|u|} \qquad \forall j \tag{21}$$

$$X_{j} \leq Z_{j,u} \qquad \forall j,u \tag{22}$$

$$Xprs_{j,t} \leq X_{j}.Mb \qquad \forall j,t \tag{23}$$

$$\sum_{j} xfc_{j,u,l,t} \geq demand_{l,u} \qquad \forall l,u \qquad (24)$$

$$Xprp_{j,u,t} \leq Capf_{j,u}.z_{j,u} \qquad \forall j,u,t \qquad (25)$$

$$Invf_{j,u,t} = Invf_{j,u,t-1} + Xprp_{j,u,t} - \sum_{l} xfc_{j,u,l,t} \qquad \forall j,u,t \qquad (26)$$

$$\sum_{u} Xprp_{j,u,t} \leq Rsp.Xprs_{j,t} + Rsc.\left(\sum_{k} xsf_{k,j,t} + \sum_{l} xcf_{l,j,t}\right) \qquad \forall j,t \qquad (27)$$

$$Invs_{k,t} = Invs_{k,t-1} + \sum_{l} xcs_{l,k,t} + Op_{k,t} - \sum_{j} xsf_{k,j,t} \qquad \forall k,t \qquad (28)$$

$$\sum_{k} xcs_{l,k,t} + \sum_{j} xcf_{l,j,t} = Rs.\sum_{j}\sum_{u} xfc_{j,u,l,t} \qquad \forall l,t \qquad (29)$$

$$Xprs_{j,t} \leq \sum_{i} xmf_{i,j,t}.Calfe_{i} \qquad \forall j,t \qquad (30)$$

$$\sum_{j} xmf_{i,j,t} \leq Capfe_{i} \qquad \forall i,t \qquad (31)$$

$$Lf_{j} = \sum_{u} z_{j,u}.Landp_{u} \qquad \forall j \qquad (32)$$

$$ych_{j,pc} \leq x_{j} \qquad \forall j,pc \qquad (33)$$

$$\sum_{pc} ych_{j,pc} \leq |pc| \qquad \forall j \qquad (34)$$

$$Lchp_{j,pc} = ych_{j,pc}.Rchp_{pc} \qquad \forall j,pc \qquad (35)$$

$$ysl_{j} \leq x_{j} \qquad \forall j \qquad (36)$$

$$Lf_{j} + \sum_{pc} Lchp_{j,pc} + Lsl_{j} \leq Landin_{j} \qquad \forall j \qquad (37)$$

$$Lsl_{j} \leq ysl_{j}.Landin_{j} \qquad \forall j \qquad (38)$$

$$zss_{j,t} \leq (\frac{2}{\pi}).zeta.Lsl_{j}.G_{max}.Ssh_{j,t}.[1+gamma.(Tm_{j,t}-T_{ref})].(\frac{720}{1000}) \qquad \forall j,t \qquad (39)$$

$$zsch_{j,t} \leq ych_{j,pc}.CHPo_{pc}.720 \qquad \forall j,t,pc \qquad (40)$$

$$Xre_{j,t} = \sum_{u} Xprp_{j,u,t}.Rep + Xprs_{j,t}.Rdr \qquad \forall j,t \qquad (41)$$

$$Slfe_{j,t} \leq zss_{j,t} + zsch_{j,t} \qquad \forall j,t \qquad (42)$$

$$Xre_{j,t} \leq Slfe_{j,t} + X_{j}.Cape_{j,t} - Rpw_{j,t} \qquad \forall j,t \qquad (43)$$

$$Rsle_{j,t} = Slfe_{j,t} + X_{j}.Cape_{j,t} - Xre_{j,t} - Rpw_{j,t} \qquad \forall j,t \qquad (44)$$

$$Inne_{t} = \sum_{j} Cape_{j,t} - \sum_{j} Xre_{j,t} - \sum_{j} Rpw_{j,t} \qquad \forall t \qquad (45)$$

$$Inns_{t} = Inne_{t} + \sum_{j} Rsle_{j,t} \qquad \forall t \qquad (46)$$

$$zw_{j,t} \geq \sum_{u} Rwt.Xprp_{j,u,t} \qquad \forall j,t \qquad (47)$$

$$zwc_{j,t} \geq Zsch_{j,t}.Rwchp_{pc} \qquad \forall j,t \qquad (48)$$

$$zw_{j,t} + zwc_{j,t} \leq Invw_{j,t} \qquad \forall j,t \qquad (49)$$

$$Invw_{j,t} = Capw_{j,t} + Rtw.zw_{j,t-1} + Invw_{j,t-1} - zw_{j,t} - zwc_{j,t} \qquad \forall j,t \qquad (50)$$

$$Zmeth_{j,t} \geq Rgs.Xprs_{j,t} \qquad \forall j,t \qquad (51)$$

$$Zmeth_{j,t} \leq Capg_{j,t} - Rg_{j,t} \qquad \forall j,t \qquad (52)$$

$$Fco_{j,t} = \sum_{u} Egs.Xprp_{j,u,t} \qquad \forall j,t \qquad (53)$$

$$CHco_{j,t} = Egsl.Zsch_{j,t} \qquad \forall j,t \qquad (54)$$

$$Trco_{t} = \left(\sum_{i}\sum_{j} dmf_{i,j}.xmf_{i,j,t} + \sum_{k}\sum_{j} dsf_{k,j}.xsf_{k,j,t} + \sum_{j}\sum_{u}\sum_{l} dfc_{j,l}.xfc_{j,u,l,t} + \sum_{l}\sum_{k} dcs_{l,k}.xcs_{l,k,t} + \sum_{l}\sum_{j} dfc_{j,l}.xcf_{l,j,t}\right).Etr \qquad \forall t \qquad (55)$$

$$\sum_{j}\sum_{u} Z_{j,u}.Emf_{j,u} + \sum_{j}\sum_{pc} ych_{j,pc}.Emch_{pc} + \sum_{j}\sum_{t} zss_{j,t}.Ems \geq Spj \qquad (56)$$

$$\text{Variables Class.1} \in \{0,1\} \qquad \forall j,u,pc \qquad (57)$$

$$\text{Variables Class.2} \geq 0 \qquad \forall i,j,l,k,t,u,pc \qquad (58)$$

$$Z_1, Z_2, Z_3 \in \Re \qquad (59)$$

Eq (21) and Eq (22) ensure that a manufacturer at location j opens only if at least one production line u is established. Eq (23) ensures that sponge iron is produced only if a manufacturer is opened at location j. Eq (24) ensures that the total amount of product u shipped from all manufacturers j to customer l in period t satisfies the corresponding demand. Eq (25) ensures that the amount of product u produced at manufacturer j in period t does not exceed its production capacity. Eq (26) defines the inventory balance of product u at each manufacturer j in period t. Eq (27) defines the required amounts of steel scrap and sponge iron for producing one ton of crude steel at manufacturer j in period t. Eq (28) defines the inventory balance of steel scrap at the scrap collection center k in period t. Equation (29) represents the trade-off between forward and reverse flows. Eq (30) Ensures that the amount of sponge iron produced by the direct reduction unit at manufacturer j in period t does not exceed the amount of iron ore supplied from suppliers i to manufacturer j in that period. Eq (31) Ensures that the amount of iron ore shipped from supplier i to manufacturer j does not exceed the supplier's capacity. Eq (32) defines the required land area for opening manufacturer j. Eq (33) allows the use of a CHP plant only if manufacturer j is open. Eq (34) ensures that the number of selected CHP plants of each type does not exceed the allowable cardinality pc. Eq (35) calculates the land area required for installing a CHP plant. Eq (36) allows a solar power plant to be opened only if manufacturer j is opened. Eq (37) calculates the total land use of all facilities, including manufacturers, CHP plants, and solar power plants. Eq (38) ensures that the land area required for the solar power plant does not exceed the available land area. Eq (39) calculates the electric power generated by the solar power plant at location j in period t. Eq (40) calculates the electric power generated by the CHP plant at location j in period t. Eq (41) defines the electricity demand of manufacturer j in period t. Eq (42) calculates the total self-generated power at location j in period t. Eq (43) ensures that the energy consumption at location j in period t does not exceed the total electricity available at that location and period. Eq (44) defines the rest of the available electricity power at location j in period t. Eq (45) defines the available electricity power at location j in period t when no on-site power generation facility is opened. Eq (46) defines the total electricity availability status at location j in period t when an on-site power generation facility is opened. Eq (47) defines the required water demand of manufacturer j in period t. Eq (48) defines the required water demand of the CHP plant at location j in period t. Eq (49) ensures that the total water consumption at location j in period t does not exceed the available water inventory. Eq (50) defines the water inventory balance at location j in period t. Eq (51) defines the natural gas demand of manufacturer j in period t. Eq (52) Ensures that the total natural gas consumption at location j in period t does not exceed its available capacity. Eq (53) calculates the total CO_2 emissions generated by manufacturer j in period t. Eq (54) calculates the total CO_2

emissions generated by the CHP plant at location j in period t. Eq (55) Calculates the total CO_2 emissions generated by transportation activities across all SC echelons in period t. Eq. (56) defines the new job-creation plan required to achieve the predefined social goal. Equations (57)-(59) define the dimensions of the decision variables.

4.1 Data-Driven Approach

Historical data are used here to parameterize seasonal energy conditions rather than to construct the robust uncertainty set. Because the optimization is multi-period and candidate locations experience different meteorological and energy-consumption patterns, location-specific polynomial regressions are fitted using supervised machine learning to estimate variations in electricity and natural-gas conditions. The fitted relationships are subsequently embedded in the optimization parameters so that monthly energy availability reflects observed meteorological-energy dependencies instead of fixed annual averages.

4.1.1. Natural gas consumption

Monthly temperature variation also affects natural-gas consumption and therefore the capacity remaining available to industrial users. Colder conditions increase heating demand and can reduce industrial gas availability, whereas warmer conditions can release network capacity. Following the location-specific temperature-consumption relationship reported by Askary et al. (2025), Eq. (62) is used to represent this seasonal effect in the gas-availability parameter.

$$G_{j,t} = (15 - 0.6471.\Delta T_{j,t}) \tag{62}$$

Accordingly, the baseline natural-gas capacity is updated through Eq. (63). Fig. 4 illustrates the observed relationship between monthly temperature and natural-gas consumption used to support this adjustment.

$$Capg_{j,t} - G_{j,t} \tag{63}$$

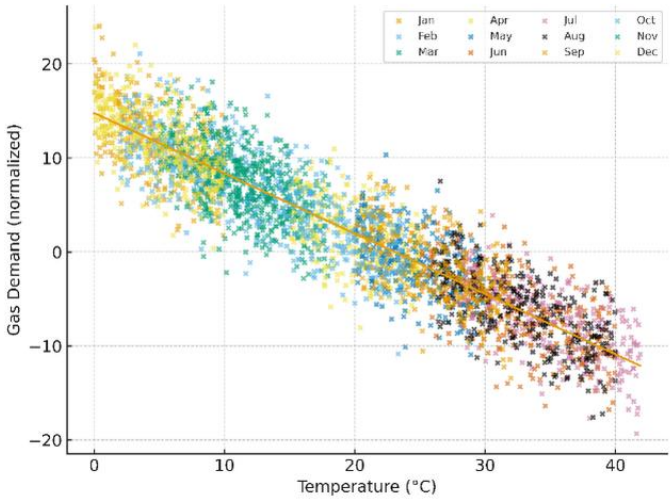


Fig. 4 Distribution of natural gas consumption data points by monthly temperature (2022-2024)

4.1.2. Meteorological variation and electricity consumption

For each candidate location, an electricity-capacity parameter represents the regional capacity remaining available for industrial supply. Because each planning period corresponds to one month, this available capacity is allowed to vary with seasonal electricity consumption and meteorological conditions. To estimate the variation, 24 years of monthly minimum and maximum temperature and daily solar-radiation data were combined with the corresponding electricity-consumption observations and fitted using location-specific polynomial regression. The resulting function is incorporated into the model through Eq. (60), replacing a time-invariant treatment of the affected electricity parameter.

$$\mathrm{Cape}_{j,t} - \Delta y_{j,t} \tag{60}$$

A separate fitted relationship is estimated for each candidate's location. Fig. 5 reports the location-specific regression behavior, while Eq. (61) represents the effect of temperature and daily sunlight variation on the corresponding electricity-consumption adjustment. These figures are intended to show how the estimated monthly electricity condition responds to the meteorological inputs used by the optimization model.

$$\Delta y_{j,t} = f_{j,t}\left(x_1, x_2 \pm 1, x_3 \pm 1, x_4 \pm 1, x_5 \pm 1\right) - f_{j,t}\left(x_1, x_2, x_3, x_4, x_5\right) \tag{61}$$

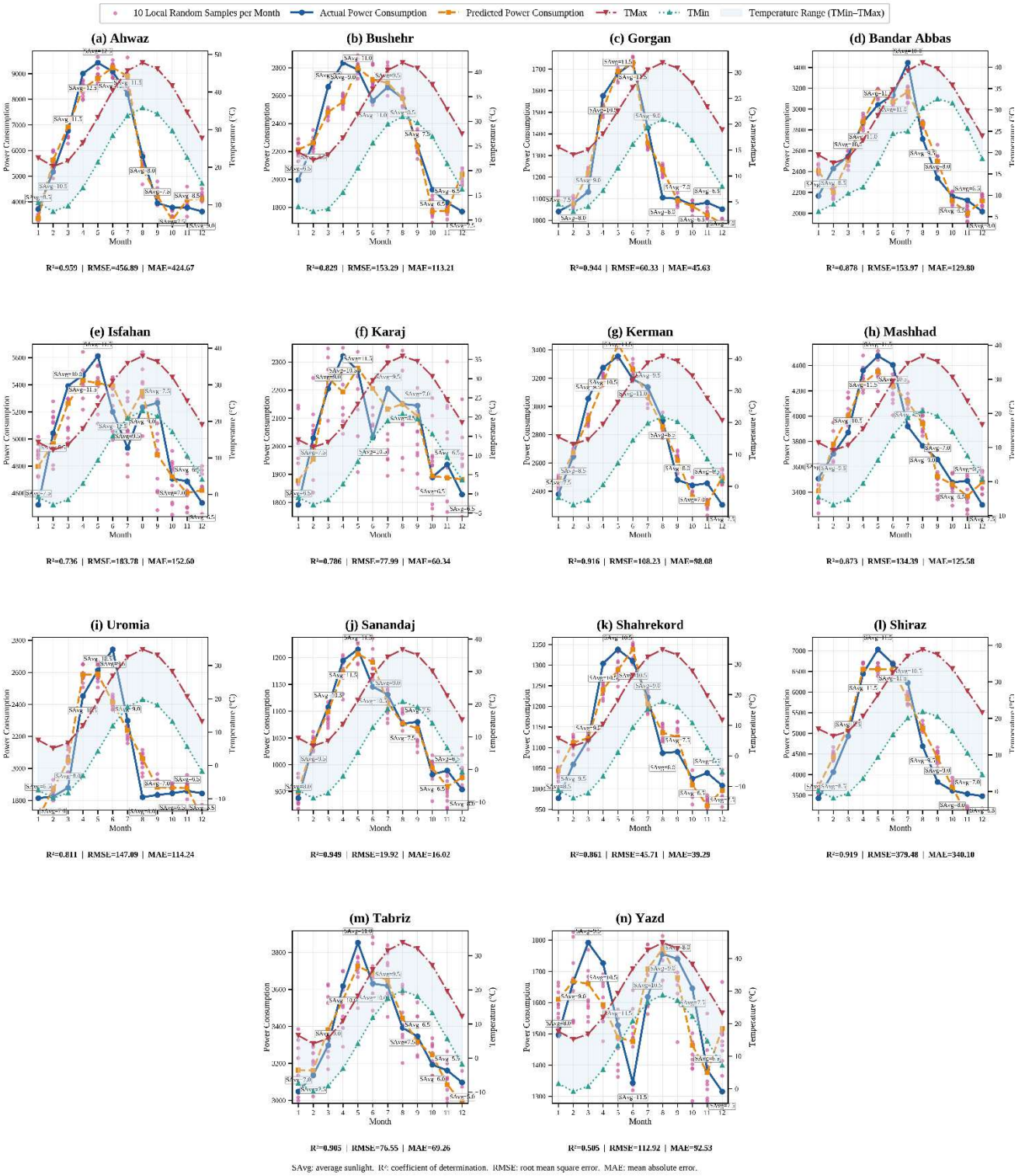


Fig. 5 City-Specific Data-Driven Prediction of Monthly Electricity Demand under Climatic Variability

4.2 Robust Optimization Under Bounded Uncertainty

For several input parameters, reliable probability distributions are not available, whereas defensible lower and upper bounds can be specified. These parameters are therefore treated as bounded interval uncertainties rather than as probabilistic random variables. Table 3 identifies the uncertain parameters and their corresponding interval representation. Robust optimization is then used to obtain strategic decisions that remain feasible against adverse realizations within the specified uncertainty set.

Table. 3 The parameters uncertainty type

Parameter	Uncertainty Nature	Definition	
$Calfe_i$	Bounded Interval Uncertainty	$[Calfe_min_i$	$Calfe_max_i]$
Tm_j	Bounded Interval Uncertainty	$[Tm_min_j$	$T_max_j]$
Ssh_j	Bounded Interval Uncertainty	$[Ssh_min_j$	$Ssh_max_j]$

To describe the robust counterpart without altering the original model structure, consider the generic linear constraint in Eq. (64), in which selected coefficients are uncertain.

$$\begin{aligned} &\min f(x) \\ &s.t: \\ &AX \le b \\ &X \ge 0 \end{aligned} \tag{64}$$

Let the uncertain members of the coefficient matrix belong to the intervals specified in Eq. (65), with the interval endpoints decomposed into nominal values and admissible deviations as subsequently defined.

$$[\bar{a}_{ij} - \hat{a}_{ij} \quad \bar{a}_{ij} + \hat{a}_{ij}] \tag{65}$$

So that:

$$\bar{a}_{ij} = \frac{a_{ij,max} + a_{ij,min}}{2} \tag{66}$$

$$\hat{a}_{ij} = \frac{a_{ij,max} - a_{ij,min}}{2} \tag{67}$$

The nominal coefficient and its disturbance term define a dimensionless perturbation variable bounded by the uncertainty set. Under this representation, the affected model constraint can be expressed in the uncertain form shown in Eq. (68).

$$\sum_j \bar{a}_{ij}.x_{ij} + \sum_{j \in j_i} \xi_{ij}.\hat{a}_{ij}.x_{ij} \le b_i \qquad \forall i \tag{68}$$

The robust requirement is that the constraint remains feasible for every admissible realization of the uncertain coefficients within the selected set. Equation (69) therefore expresses the corresponding worst-case protection condition.

$$\sum_j \bar{a}_{ij}.x_{ij} + \max_{\xi \in U} \left(\sum_{j \in j_i} \xi_{ij}.\hat{a}_{ij}.x_{ij} \right) \le b_i \qquad \forall i \tag{69}$$

Different robust counterparts result from different uncertainty-set geometries (Li et al., 2011). This study uses a box uncertainty set, represented by the infinity-norm condition in Eq. (70), to bound simultaneous coefficient deviations within the normalized protection region.

$$U_{\infty} = \left\{ \xi \middle\| \xi \right| \le \Psi, \forall j \in j_i \right\} \tag{70}$$

The parameter controls the protection level within the normalized uncertainty set used in this study. =0 reproduces the nominal deterministic case, while larger values within the adopted range [0,1] increase protection against adverse deviations and may therefore increase conservatism. Replacing the inner worst-case term by its equivalent robust form yields Eq. (71).

$$\sum_j \bar{a}_{ij}.x_{ij} + \Psi.\sum_{j \in j_i} \hat{a}_{ij}.x_{ij} \le b_i \qquad \forall i \tag{71}$$

This robustification procedure is applied to model constraints containing the selected uncertain parameters. For iron-ore grade, the uncertain form associated with Eq. (71) is written as Eq. (72).

$$Xprs_{j,t} \le \sum_i xmf_{i,j,t}.Calfe_i \tag{72}$$

The resulting robust counterpart is given in Eq. (73).

$$Xprs_{j,t} \le \sum_i xmf_{i,j,t}.\left(\frac{Calfe_max_i + Calfe_min_i}{2} \right) + \psi_1.\left[\sum_i xmf_{i,j,t}.\left(\frac{Calfe_max_i - Calfe_min_i}{2} \right) \right] \tag{73}$$

The second affected relationship is robustified in the same manner because its selected parameters are represented by bounded uncertainty, leading from Eq. (74) to the robust counterpart in Eq. (75).

$$Zss_{j,t} \le \left(\frac{2}{\pi}\right).zeta.Lsl_j.G_{max}.Ssh_{j,t}.[1+gamma.(Tm_{j,t}-T_{ref})].\left(\frac{720}{1000}\right) \tag{74}$$

The robust counterpart is therefore represented by Eq. (75).

$$\begin{aligned} Zss_{j,t} \le{}& \left(\frac{2}{\pi}\right).zeta.Lsl_j.G_{max}.\left(\frac{Ssh_max_{j,t} + Ssh_min_{j,t}}{2} \right).[1+gamma.(\left(\frac{Tm_max_{j,t} + Tm_min_{j,t}}{2} \right)-T_{ref})].\left(\frac{720}{1000}\right) \\ &+\psi_2 \left[\left(\frac{2}{\pi}\right).zeta.Lsl_j.G_{max}.\left(\frac{Ssh_max_{j,t} - Ssh_min_{j,t}}{2} \right).[1+gamma.(\left(\frac{Tm_max_{j,t} - Tm_min_{j,t}}{2} \right)-T_{ref})].\left(\frac{720}{1000}\right) \right] \end{aligned} \tag{75}$$

4.3 Raw material cost

Iron ore is the primary feedstock for direct-reduction production, and its iron content varies across suppliers and mining regions. Because lower-grade ore contains less usable iron, supplier quality influences both the material requirement and the economic attractiveness of procurement. In the model, the iron-ore purchasing cost is therefore parameterized as a function of supplier iron grade: higher-purity material is assigned a higher unit procurement price, whereas lower-grade material has a lower unit price but may require greater material input through the production balance. Equation (76) defines this grade-dependent purchasing-cost relationship. The CDM parameter is specified by the decision maker and controls the intensity of the grade-related price adjustment.

$$\text{Total cost for iron Ore in supplier (i)} = \text{Orc}_i + \left[\left(\frac{\text{Calfe_max}_i + \text{Calfe_min}_i}{2}\right) + \psi_3 \cdot \left(\frac{\text{Calfe_max}_i - \text{Calfe_min}_i}{2}\right) - 0.55\right].\text{CDM} \quad (76)$$

5. Case Study and Computational Results

A real-world steel supply-chain expansion problem in Iran is used to evaluate the proposed framework. Candidate facilities represent DRI-EAF steelmaking systems with direct reduction, pellet-related feed preparation, electric-arc-furnace processing, and continuous casting. Table 4 reports the network dimensions, including suppliers, candidate plants, customers, monthly periods, scrap centers, products, and on-site generation alternatives.

Table. 4 Specification of supply chain components

Iron Ore Supplier	Potential Manufacturer	Consumer	Period (Month)	Steel Scrap Center	Products	Type Of Self-Sustained
10	14	70	12	14	3	4

The model is implemented in GAMS (version 2.8.24/64-bit) and solved with CPLEX on an Intel Core i7 2.6-GHz computer with 8 GB RAM. Because the formulation contains three conflicting objectives, the augmented epsilon-constraint method is used to generate nondominated solutions (Askary et al., 2025). The total-cost objective is treated as the master objective, while the bounds associated with the grid-export and CO_2 objectives are varied over their admissible ranges to generate the Pareto set. Fig. 6 shows the optimal model configuration including locations, land use allocations, on site generation position, and number of site selections which the Tables 5 and 6 show the their detailed. The case-study solve complete computation required approximately 21.h to generate nondominated solution (global optimization). Optimal results related to proposed model reports as following subsection.

Table.5 Optimal locations to open the facility

	Facility													
Product	1	2	3	4	5	6	7	8	9	10	11	12	13	14
Bloom	Y	N	Y	Y	N	Y	Y	N	Y	N	N	N	N	Y
Billet	Y	N	Y	Y	N	Y	Y	N	Y	N	N	N	N	Y
Slab	Y	N	Y	Y	N	Y	Y	N	Y	N	N	N	N	Y

Y: Open N: Close

Table.6 Optimal land allocation based on different activity (m^2)

	Facility						
Specification	1	3	4	6	7	9	14
Manufacturing	255000	255000	255000	255000	255000	255000	255000
Solar Plant	345000	845000	2345000	1845000	2845000	1345000	1445000
CHP Plant	900000	900000	900000	900000	900000	900000	900000
Total Land Use	1500000	2000000	3500000	3000000	4000000	2500000	2600000



Fig. 6 Optimal results for case study

5.1 Energy scope report

To pay for native electricity supply reliability, Fig.7 demonstrates the adaptive energy-balancing capability of the proposed system. Although the regression-based grid injection ceiling supplies only 47.6-58.4% of monthly demand, coordinated solar and CHP generation raises the available supply to 100.06-102.05% of demand, eliminating grid-induced deficits in all 12 months. This dynamic complementarity enables the proposed design to maintain energy adequacy despite substantial seasonal variations in both load and grid availability. Fig. 8 demonstrates a reliability-induced economic crossover: increasing grid disruption rapidly erodes the cost advantage of the traditional system, whereas the proposed configuration remains comparatively resilient through on-site generation. Once outage exposure exceeds 38.68%, the proposed design becomes economically dominant, yielding up to 224.5 trillion Rial/year in avoided system cost. Fig. 9 exposes the structural vulnerability of grid-dependent production to coupled climate and demand variability. Climate derating reduces monthly grid availability by 14.6-26.6 GWh, while the grid-only deficit escalates to 332.8-507.6 GWh, peaking during high-load months. In contrast, the proposed system eliminates the post-on-site deficit across all months, demonstrating that self-generation acts as an effective resilience buffer against both climate-induced derating and seasonal grid inadequacy. As shown in Fig. 10, integrating a 15% scrap share reduces annual natural-gas demand from 1,972.35 to 1,676.50 Mm^3, saving 295.85 Mm^3 and reinforcing the energy-resilience advantage of the proposed system.

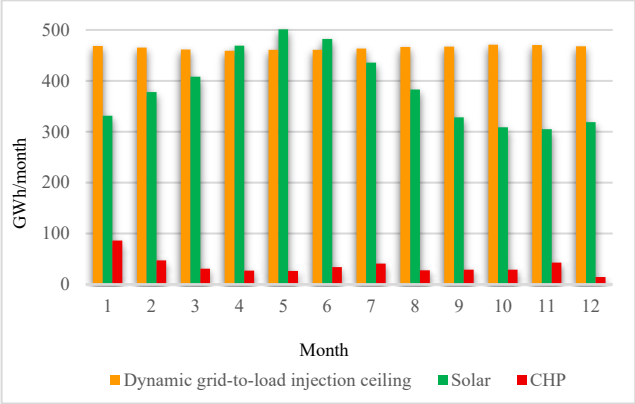


Fig . 7 Dynamic monthly energy adequacies

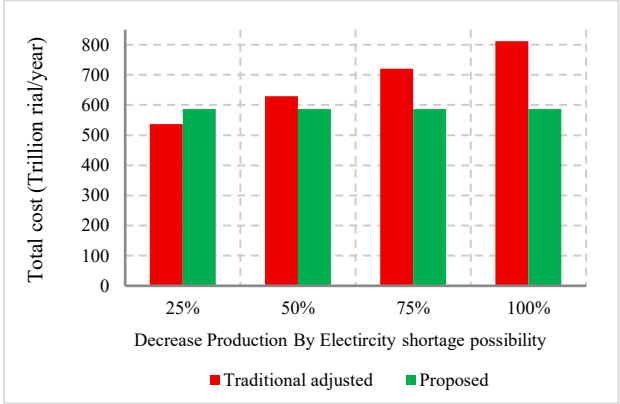


Figure 8. Reliability-driven cost considering lines idle

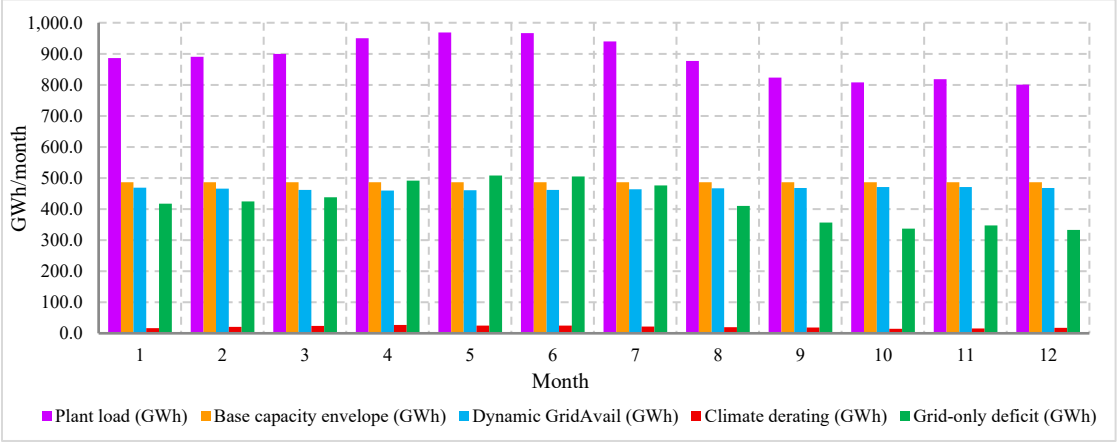


Fig. 9 Climate-driven grid deficit and resilience

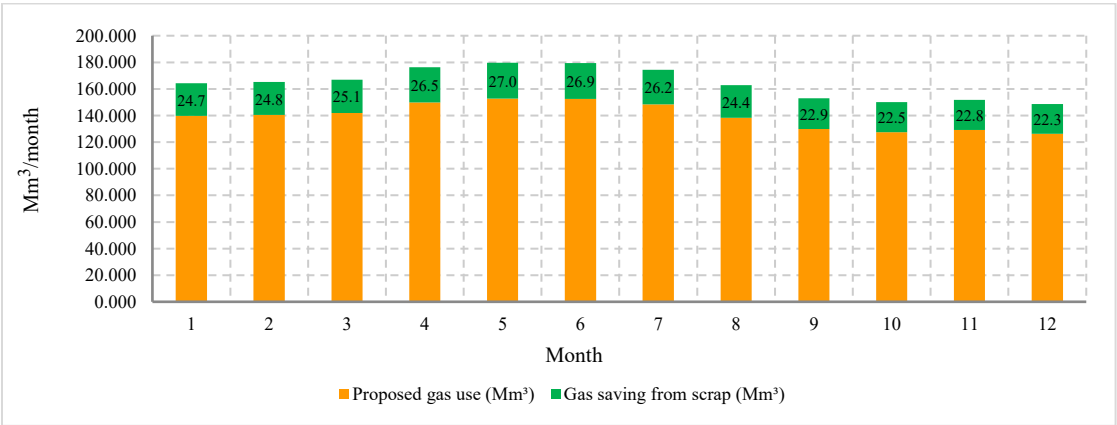


Fig. 10 Dynamic monthly natural-gas demand and scrap-induced savings

5.2. Supply Chain Scope Report

The 12-month production and inventory trajectories are shown in Figs. 11 and 12. Their joint interpretation is more informative than either series: when production falls in selected months, previously accumulated inventory is used to maintain demand satisfaction rather than forcing additional production under less favorable resource conditions. This intertemporal substitution provides the model with

operational flexibility and helps coordinate production with monthly electricity availability and the environmental objective.

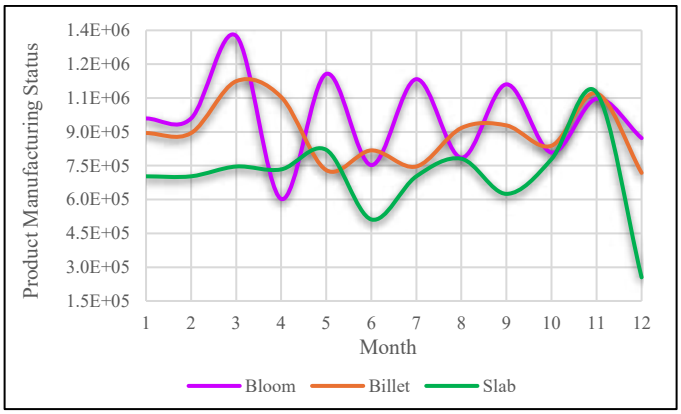


Fig. 11 Optimal manufacturing for each product per month

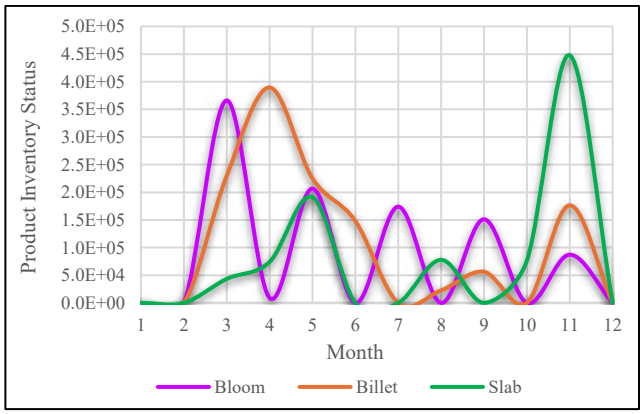


Fig. 12 Optimal manufacturing for each product per month

5.3. CO_2 Reduction Scope Report

As summarized in Table 7, the proposed model reduces total CO_2 emissions by approximately 6.2% relative to the Traditional configuration. The largest reduction is observed in transport emissions (54.5%), reflecting the optimized network structure, while scrap integration lowers natural-gas combustion emissions by 15.0%. Replacing CHP-based electricity with solar generation eliminates the corresponding operational CO_2 emissions, whereas the upstream effect associated with lower iron-ore use remains comparatively limited (0.3%). Overall, the results show that the main decarbonization benefits arise from network optimization, scrap utilization, and renewable on-site power generation.

Table. 7 Compare the CO_2 emission pollution of proposed model vs traditional

Indicator	Traditional	Proposed	Percentage
Full Model	2.47	2.31	-6.2%
Transport CO_2	0.28	0.12	-54.5%
Natural-gas combustion	0.33	0.27	-15.0%
CHP replace with Solar	0.14	0	-100.0%
Iron-ore upstream context	0.01578	0.01574	-0.3%

5.4. Circular Economic Scope Report

Table 8 demonstrates that the proposed model transforms circularity from an isolated recovery practice into an integrated resource-efficiency strategy. Compared with the Traditional configuration, the model reduces natural-gas use by 24.654 Mm^3/y, electricity demand by 27.394 GWh/y, grid dependence by 206.818 GWh/y, and fresh-water withdrawal by 12.327 Mm^3/y, while simultaneously supplying 20.26% of electricity demand through on-site renewable generation. In parallel, the closed-loop material structure incorporates 0.274 Mt/y of scrap, equivalent to 15% of steel output, thereby reducing reliance on virgin inputs. These results indicate that the principal contribution of the proposed design is not a single-resource

saving, but the simultaneous closure of material, water, and energy loops within one optimized supply-chain architecture.

Table 8 Circular economic benefit of proposed model related to traditional model

Circular dimension	Indicator	Traditional	Proposed	Absolute change	Unit	Circular mechanism
Energy	Natural-gas demand	164.363	139.708	-24.654	Mm^3/y	Scrap-driven DRI displacement
Energy	Electricity demand	913.125	885.731	-27.394	GWh/y	Scrap-driven energy saving
Energy	Grid electricity	913.125	706.307	-206.818	GWh/y	On-site solar substitution
Energy	On-site energy coverage	0.000	20.257	20.257	% of demand	Renewable self-supply
Energy	Fresh-water demand	16.436	4.109	-12.327	Mm^3/y	Wastewater recovery and reuse
Materials	Steel scrap input	0.000	0.274	0.274	Mt/y	Closed-loop scrap recovery
Materials	Scrap share	0.000	15.000	15.000	% of steel	Secondary-material substitution
Materials	Virgin iron ore	3.215	3.207	-0.009	Mt/y	Virgin-material displacement

6. Integrated Performance Assessment and Managerial Implications

Table 14 consolidates the principal system-level outcomes derived from the selected optimization solution and the post-optimization conversion factors reported by the cited industry sources. The indicators should be interpreted as consequences of the integrated network design rather than as independent benefits. In particular, scrap recovery reduces primary-material requirements and associated resource use; optimal land allocation enables a combination of manufacturing and on-site generation; wastewater treatment reduces fresh-water dependence; and surplus on-site electricity creates a potential grid-support contribution. For managerial use, the results imply that steel producers, industrial-zone authorities, and energy planners should evaluate candidate expansion sites jointly rather than sequentially. A site with limited grid capacity need not be rejected automatically if sufficient industrial land and on-site generation options are available, but allocating land to energy infrastructure has an explicit opportunity cost because the same land cannot simultaneously support additional production capacity. The framework is therefore most useful where electricity constraints, heterogeneous regional resources, and finite industrial land materially affect capacity-expansion decisions.

7. Nondominated Solutions, Verification, and Validation

This section evaluates whether the formulation exhibits internally consistent optimization behavior and whether its central energy-security mechanism performs as intended. The analysis combines objective-trade-off assessment, parameter sensitivity tests, a counterfactual test of on-site generation, and out-of-sample comparison of deterministic and robust policies.

7.1 Conflict Among Objective Functions

The tri-objective model generates a set of Pareto-optimal or nondominated alternatives rather than a single universally optimal solution. Fig. 13 shows the trade-off between total system cost and surplus on-site electricity supplied to the grid: increasing grid support requires additional investment or operating expenditure, whereas stronger cost minimization limits the amount of surplus electricity available for export. Fig. 14 shows the corresponding trade-off between the grid-export objective and the CO_2 objective. Higher on-site electricity export can increase emissions when additional dispatchable CHP generation is

required, whereas stronger emission minimization favors a lower-emission energy mix and may reduce exportable surplus. The Pareto set therefore makes the economic-energy-environmental consequences of the design explicit and allows the decision maker to select a nondominated solution according to policy priorities rather than obscuring these conflicts in a single weighted objective.

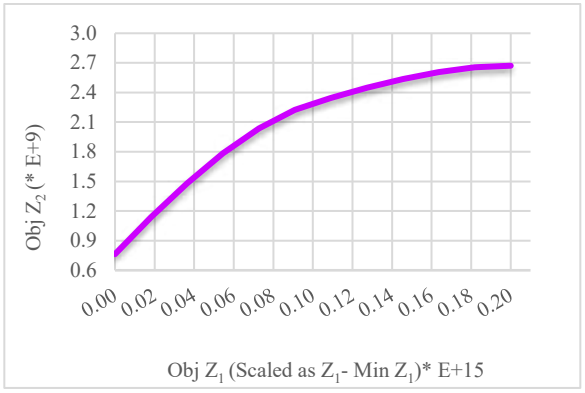


Fig. 13 Nondominated points (maximizing second obj vs minimizing first obj)

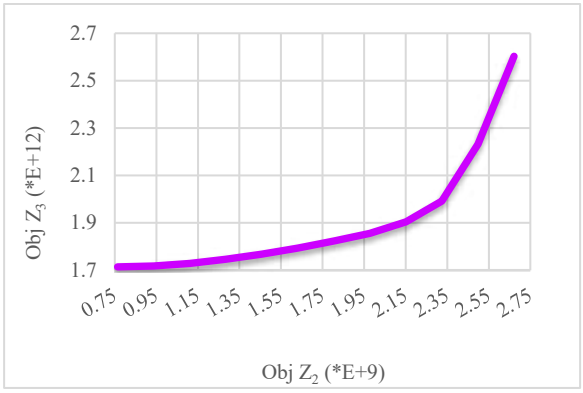


Fig. 14 Nondominated points (maximizing second obj vs minimizing third obj)

7.2 Model Verification

Sensitivity analysis is used to verify the direction and internal logic of key model responses without altering the calibrated case-study results. Increasing the crude-steel CO_2 emission factor raises total emissions (Fig. 15), and increasing the electricity requirement per ton raises aggregate electricity consumption (Fig. 16). Higher iron-ore grade reduces the quantity of ore required for a given production target (Fig. 17). Increasing available grid capacity reduces the need for on-site generation (Fig. 18), which directly supports the model's energy-substitution logic. When monthly electricity requirements increase, the model responds primarily by expanding solar generation, while CHP generation changes more modestly (Fig. 19), reflecting the interaction between energy adequacy and the CO_2 objective. Finally, higher inventory holding cost reduces the optimal inventory level (Fig. 20). Taken together, these experiments show that the model responds in the expected economic, material, energy, and environmental directions.



Fig. 15 Environmental objective function to increasing Egs parameter

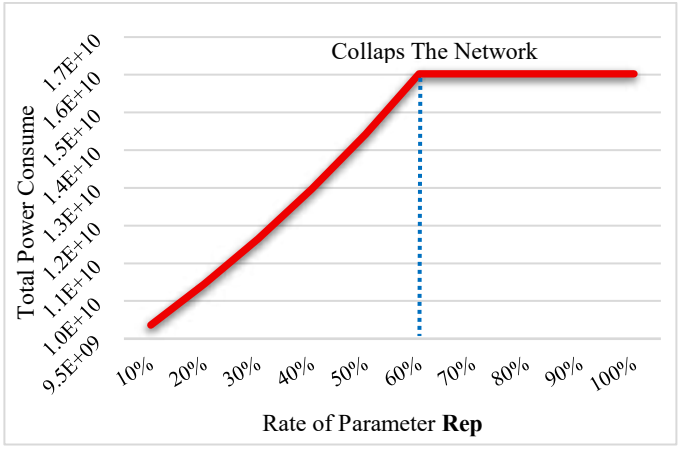


Fig. 16 Electrical energy consumption to increasing Rep parameter

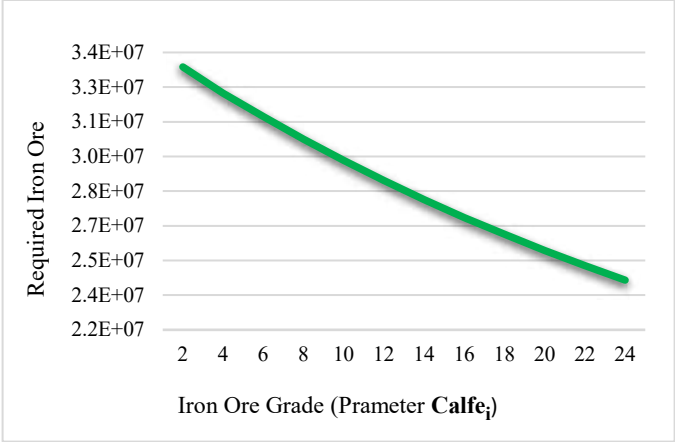


Fig. 17 Iron ore requirement for crude steel production with increasing ore grade

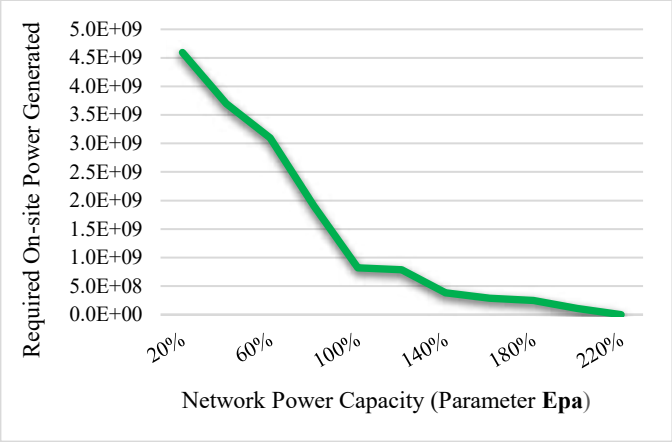


Fig. 18 Require on-site power generation with increasing grid capacity

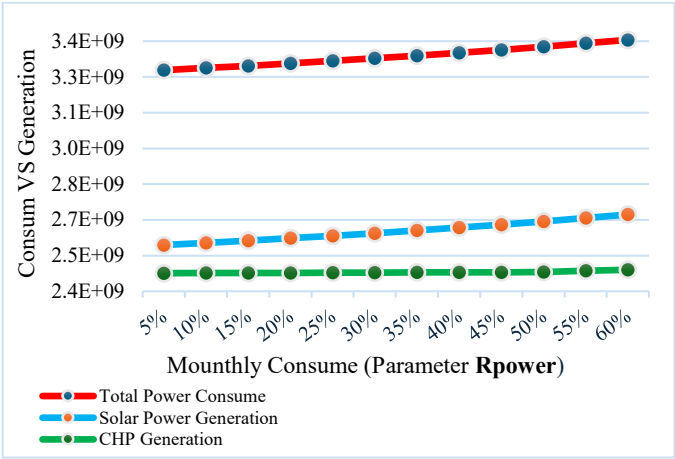


Fig. 19 On-site energy generation with increasing monthly consumption rate

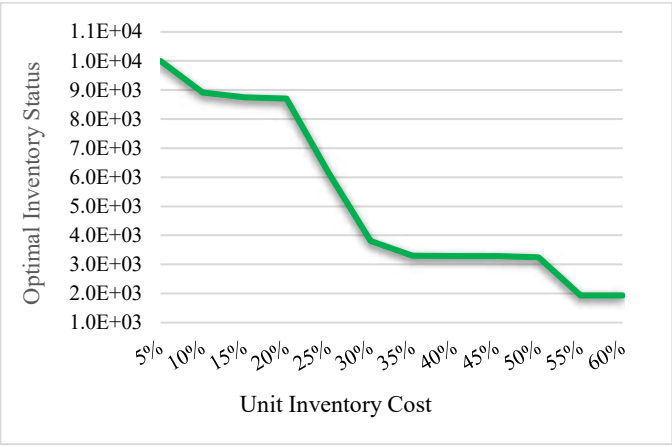


Fig. 20 Annual product inventory levels with increasing unit holding cost

7.4 Validation Through Robust Optimization

The practical effect of uncertainty protection is evaluated by comparing the deterministic policy with robust policies at Ψ=0, 0.25, 0.50, 0.75, and 1.00. Strategic decisions are fixed for each policy and evaluated under the same out-of-sample realizations, while operational decisions are allowed to adapt to each realization. Fig. 21 shows that the deterministic policy and the robust policy at Ψ =0 coincide, as expected, and that the mean realized cost increases gradually as protection strengthens. This increase is the economic premium paid for greater protection against adverse parameter deviations. Fig. 22 shows an overall reduction in the dispersion of realized cost, from approximately 1.79 in the deterministic case to 1.78, 1.75, 1.76, and 1.74 across the successive robust levels. The small intermediate increase between Ψ =0.50 and Ψ=0.75 means that the reduction is not strictly monotonic, but the overall trend indicates improved stability at higher protection. Fig. 23 reports the corresponding price of robustness, which increases as the model adopts more conservative protection levels. Together, these results demonstrate the expected cost-stability trade-off of the robust formulation.

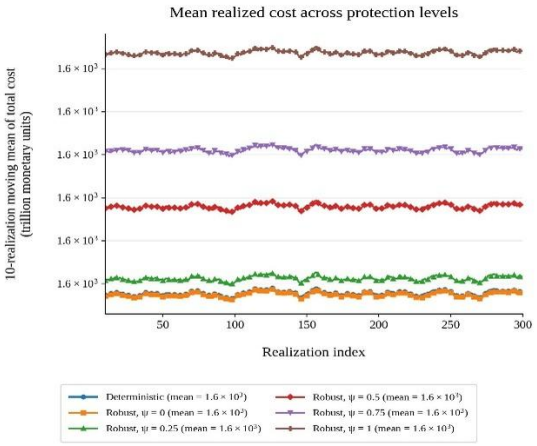


Fig. 21 Mean of total cost for the deterministic policy and robust policies under protection levels ψ

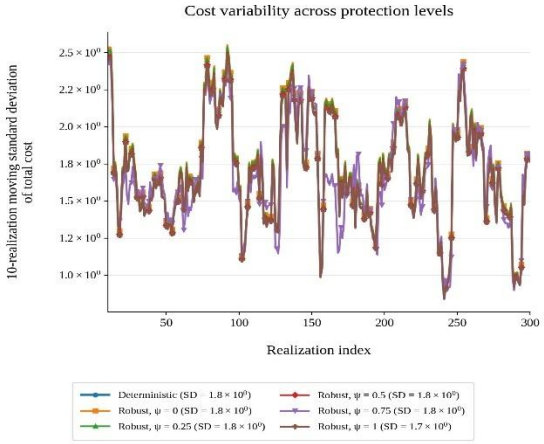


Fig. 22 Standard deviation of total cost for the deterministic policy and robust policies under protection levels ψ

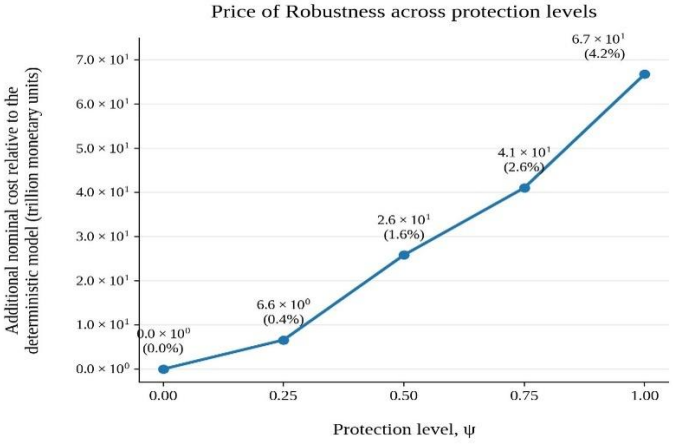


Fig. 23 Price of Robustness across protection levels ψ

8. Conclusion

This study developed a robust, sustainable, closed-loop steel supply-chain design framework in which steel-production capacity and on-site electricity generation are co-planned under finite industrial land and heterogeneous regional resource constraints. The central contribution is the endogenous land-energy-production coupling: manufacturing lines, solar PV, and CHP units compete for a common land resource, allowing the model to determine whether an electricity-constrained but otherwise attractive site can remain feasible through on-site generation. Historical meteorological and energy data are used to estimate location- and month-specific energy conditions, while bound robust optimization protects strategic decisions against adverse parameter deviations. Scrap recovery, wastewater reuse, CO_2 emissions, grid export, and employment requirements are integrated to quantify the broader sustainability implications of the selected design. The real-world case study demonstrates that the selected network generates approximately 1.29E+10 kWh of on-site electricity annually, including 6.94E+9 kWh from solar PV, and exports approximately 5.34E+9 kWh of surplus on-site electricity to the grid. The circular-resource strategy avoids

approximately 6.1E+6 t of iron-ore extraction, contributes to approximately 2.8E+9 kg/year of reported CO_2 mitigation, and supports substantial reductions in natural-gas, electricity, and freshwater requirements, while the integrated recycling and on-site-energy plan creates 7,415 jobs. More importantly, the land-allocation results show that energy security is not separable from capacity planning: when industrial land is scarce, the feasibility and value of additional production depend on how much of that same land must be reserved for energy infrastructure. The framework is therefore most applicable to energy-constrained industrial regions where facility location, power adequacy, and land availability must be decided jointly. Future research can extend the system boundary to thermal recovery from CHP, electricity storage, endogenous grid-export pricing, alternative low-carbon generation technologies, and richer data-derived uncertainty sets while preserving the integrated land-energy-production decision structure.

Declarations

1. Data availability statement:

The underlying case-study datasets analyzed during the current study are not publicly available due to confidentiality and security-related restrictions associated with the study context. The data necessary for verification of the reported analyses can be made available to the Scientific Reports Editorial Board Members, Dear reviewers, and referees upon request, solely for the purpose of manuscript evaluation and subject to the applicable confidentiality restrictions. The non-confidential aggregated results are reported in the tables and figures of this article.

2. Disclosure statement:

The authors report there are no competing interests to declare.

3. Funding:

None.

4. Declaration of generative AI use:

AI was used to check English grammar.

Reference:

Almeida, J. F. F., Conceição, S. V., Pinto, L. R., Oliveira, B. R. P., & Rodrigues, L. F. (2022). Optimal sales and operations planning for integrated steel industries. *Annals of Operations Research*, *315*(2), 773-790.

Askary, M., Aliha, M. R. M., Makui, A., & Pishvaee, M. S. (2025). Robust green supply chain for flare waste gas recycling under hybrid uncertainty: A data-driven approach. *Energy*, 139642.

Amasyali, K., & El-Gohary, N. M. (2018). A review of data-driven building energy consumption prediction studies. Renewable and Sustainable Energy Reviews, 81, 1192-1205.

Al-Refaie, A., Jarrar, Y., & Lepkova, N. (2021). Sustainable design of a multi-echelon closed loop supply chain under uncertainty for durable products. *Sustainability*, *13*(19), 11126.

Afroozi, M. A., Gramifar, M., Hazratifar, B., Keshvari, M. M., & Razavian, S. B. (2025). Optimization of Lithium-Ion Battery Circular Economy in Electric Vehicles in Sustainable Supply Chain. *Battery Energy*, *4*(2), e20240057.

Askary, M., Makui, A., & Tajik, M. (2024). A robust multi-objective MIP model to optimize the supply chain of steel industry taking into account the sustainability approach. *RAIRO-Operations Research*, *58*(2), 1059-1091.

Abdelsattar, M., Ismeil, M. A., Aly, M. M., & Abu-Elwfa, S. S. (2024). Energy management of microgrid with renewable energy sources: A case study in Hurghada Egypt. *IEEE Access*, *12*, 19500-19509.

Alharairi, M., Amin, S. H., & Zolfaghari, S. (2026). A new multi-objective optimization model for Carinata-based sustainable aviation fuel supply chain network design. *Applied Energy*, *414*, 127764.

Amin, S. H., & Baki, F. (2017). A facility location model for global closed-loop supply chain network design. Applied Mathematical Modelling, 41, 316-330.

Ahmed, M., Al Amareen, O. S., & Arafat, Y. (2026). Harnessing big data for reverse logistics and waste management: Pathways to sustainable supply chains. In *Enhancing Sustainability in Global Supply Chains With Big Data Analytics* (pp. 175-210). IGI Global Scientific Publishing.

Askary, M., Makui, A., & Aliha, M. R. M. (2025, October). Optimization of the vehicle soft-routing model: effect of the route third dimension on the transportation costs and travelled route shape. In Operations Research Forum (Vol. 6, No. 4, p. 147). Cham: Springer International Publishing.

Becerra, P., Mula, J., & Sanchis, R. (2024). Optimising location, inventory and transportation in a sustainable closed-loop supply chain. *International Journal of Production Research*, *62*(5), 1609-1632.

Baghizadeh, K., Pahl, J., & Hu, G. (2021). Closed-loop supply chain design with sustainability aspects and network resilience under uncertainty: Modelling and application. *Mathematical Problems in Engineering*, *2021*(1), 9951220.

Chen, L., Dong, T., Peng, J., & Ralescu, D. (2023). Uncertainty analysis and optimization modeling with application to supply chain management: A systematic review. *Mathematics*, *11*(11), 2530.

Chang, N. L., Dehghanimadvar, M., & Egan, R. (2022). The cost of risk mitigation—Diversifying the global solar PV supply chain. *Joule*, *6*(12), 2686-2688.

Duffie, J. A., & Beckman, W. A. (2013). *Solar Engineering of Thermal Processes* (4th ed.). Wiley.

Ding, H., Feng, M., & Chen, Q. (2025). How supply chain disruptions, renewable energy consumption, and eco-innovation mitigate environmental degradation? A path towards sustainable development in France. *Energy Economics*, *145*, 108346.

de Vries-Gao, A. (2025). Artificial intelligence: Supply chain constraints and energy implications. *Joule*, *9*(6).

Darabad, S. D., Ghannadpour, S. F., Noori, S., & Bagherpour, M. (2025). LeanVironment meets Greenpulse: optimizing sustainable multi-project construction supply chains. *Environment, Development and Sustainability*, 1-48.

Emodi, N. V., Chaiechi, T., & Alam Beg, A. R. (2018). The impact of climate change on electricity demand in Australia. Energy & Environment, 29(7), 1263-1297.

Fasihi, M., Tavakkoli-Moghaddam, R., Hajiaghaei-Keshteli, M., & Najafi, S. E. (2023). Designing a sustainable fish closed-loop supply chain network under uncertainty. *Environmental science and pollution research*, *30*(39), 90050-90087.

Fuhrlaender, D., Vermeulen, B., & Schnuelle, C. (2025). Green hydrogen transformation of the iron and steel production system: An integrated operating concept for system-internal balance, lower emissions, and support for power system stability. *Applied Energy*, *381*, 125104.

Farajiamiri, M., Meyer, J. C., & Walther, G. (2023). Multi-objective optimization of renewable fuel supply chains regarding cost, land use, and water use. *Applied Energy*, *349*, 121652.

Fan, Z., & Friedmann, S. J. (2021). Low-carbon production of iron and steel: Technology options, economic assessment, and policy. *Joule*, *5*(4), 829-862.

Gao, Y., Lu, S., Cheng, H., & Liu, X. (2024). Data-driven robust optimization of dual-channel closed-loop supply chain network design considering uncertain demand and carbon cap-and-trade policy. Computers & Industrial Engineering, 187, 109811.

Gilani, H., & Sahebi, H. (2022). A data-driven robust optimization model by cutting hyperplanes on vaccine access uncertainty in COVID-19 vaccine supply chain. *Omega*, *110*, 102637.

Gholian-Jouybari, F., Hashemi-Amiri, O., Mosallanezhad, B., & Hajiaghaei-Keshteli, M. (2023). Metaheuristic algorithms for a sustainable agri-food supply chain considering marketing practices under uncertainty. *Expert systems with applications*, *213*, 118880.

Giri, B. K., & Roy, S. K. (2024). Fuzzy-random robust flexible programming on sustainable closed-loop renewable energy supply chain. *Applied Energy*, *363*, 123044.

Garrido-Perez, J. M., Barriopedro, D., García-Herrera, R., & Ordóñez, C. (2021). Impact of climate change on Spanish electricity demand. Climatic Change, 165(3), 50.

Harpprecht, C., Sacchi, R., Naegler, T., van Sluisveld, M., Daioglou, V., Tukker, A., & Steubing, B. (2025). Future environmental impacts of global iron and steel production. Energy & Environmental Science, 18(16), 8009-8028.

Hosseini, F., Barzinpour, F., & Askary, M. (2025). Designing sustainable perishable food supply chain under disruption risks: A case study of dairy products. *Journal of Industrial and Systems Engineering*, *17*(2), 197-220.

Khot, S. B., & Thiagarajan, S. (2024). Developing a resilient and sustainable non-linear closed-loop supply chain management framework for the automotive sector industry using a gaussian fuzzy optimization based non-linear model predictive control approach. *Journal of Industrial and Production Engineering*, *41*(2), 101-120.

Jin, S., Liu, Q., Zhang, W., He, Z., He, Y., Zhang, L., ... & He, Y. (2023). Data-driven methods for situation awareness and operational adjustment of sustainable energy integration into power systems. Frontiers in Energy Research, 11, 1253206.

Li, B., Gao, D., Zhang, C., Yu, Z., Stolterfoht, M., Lin, Y. H., ... & Zhu, Z. (2026). Closed-loop manufacturing for sustainable perovskite photovoltaics. *Nature Reviews Materials*, *11*(1), 10-25.

Lotfi, R., Bazregar, M., Ali, S. S., Farbod, E., Aghakhani, S., & Meymandi, Z. R. (2025). Synergistic Closed-Loop Supply Chain Network Design by Considering Robustness, Risk: An Automotive Case Study. *Engineering Reports*, *7*(3), e70010.

Mohammadi, M., & Nikzad, A. (2023). Sustainable and reliable closed-loop supply chain network design during pandemic outbreaks and disruptions. *Operations management research*, *16*(2), 969-991.

Meyer, B. H., Prescott, B. C., & Sheng, X. S. (2023). The impact of supply chain disruptions on business expectations during the pandemic. *Energy Economics*, *126*, 106951.

Moghadam, S. S., Gholamian, M. R., Zahedi, R., & Shaqaqifar, M. (2024). Designing a multi-purpose network of sustainable and closed-loop renewable energy supply chain, considering reliability and circular economy. *Applied Energy*, *369*, 123539.

Min, J., Dong, Y., & Wang, H. (2022). Response of Natural Gas Consumption to Temperature and Projection under SSP Scenarios during Winter in Beijing. Atmosphere, 13(8), 1178.

Mohammadi, Z., Barzinpour, F., & Teimoury, E. (2023). A location-inventory model for the sustainable supply chain of perishable products based on pricing and replenishment decisions: A case study. *PloS one*, *18*(7), e0288915.

Na, H., Qiu, Z., Sun, J., Yuan, Y., Zhang, L., & Du, T. (2024). Revealing cradle-to-gate CO_2 emissions for steel product producing by different technological pathways based on material flow analysis. *Resources, Conservation and Recycling*, *203*, 107416.

Nikian, A., Khademi Zare, H., Lotfi, M. M., & Fallah Nezhad, M. S. (2023). Redesign of a sustainable and resilient closed-loop supply chain network under uncertainty and disruption caused by sanctions and COVID-19. *Operations management research*, *16*(2), 1019-1042.

Petrova, T. S., Vladova, R. K., & Kirilova, E. G. (2023). A robust optimisation model for the sustainable design of a dairy supply chain under uncertain environmental conditions. *Chemical Engineering Transactions*, *103*, 853-858.

Panjehpour, A., & Zarrinpoor, N. (2025). A network design of a canola-to-biodiesel supply chain by considering the water-energy-food-land-ecosystem-undesirable climate change nexus. *Computers & Industrial Engineering*, *199*, 110610.

Pinto, J. T., & Diemer, A. (2020). Supply chain integration strategies and circularity in the European steel industry. *Resources, Conservation and Recycling*, *153*, 104517.

Razavi, N., Gholizadeh, H., Nayeri, S., & Ashrafi, T. A. (2021). A robust optimization model of the field hospitals in the sustainable blood supply chain in crisis logistics. *Journal of the Operational Research Society*, *72*(12), 2804-2828.

Rani, A., Singh, S. K., Goel, A., & Chauhan, A. (2025). Sustainable food waste-to-bioenergy supply chain with rate of return under triple bottom line approach. *Applied Energy*, *399*, 126454.

Ren, M., Lu, P., Liu, X., Hossain, M. S., Fang, Y., Hanaoka, T., ... & Dai, H. (2021). Decarbonizing China's iron and steel industry from the supply and demand sides for carbon neutrality. *Applied Energy*, *298*, 117209.

Shen, J., Zhang, Q., & Tian, S. (2025). Decarbonization pathways analysis and recommendations in the green steel supply chain of a typical steel end user-automotive industry. *Applied Energy*, *377*, 124711.

Shakuri, M., & Barzinpour, F. (2024). A risk-averse sustainable perishable food supply chain considering production and delivery times with real-world application. *Plos One*, *19*(9), e0308332.

Shaker, L. M., Al-Amiery, A. A., Hanoon, M. M., Al-Azzawi, W. K., & Kadhum, A. A. H. (2024). Examining the influence of thermal effects on solar cells: a comprehensive review. *Sustainable Energy Research*, *11*(1), 6.

Staffell, I., Pfenninger, S., & Johnson, N. (2023). A global model of hourly space heating and cooling demand at multiple spatial scales. *Nature Energy*, *8*(12), 1328-1344.

Shahabuddin, M., Akbar Rhamdhani, M., Brooks, G., Fontana, A., & King, A. (2024). Substituting natural gas with hydrogen: A case study on mass, energy, and emissions in electric arc furnace steelmaking. *Ironmaking & Steelmaking*, *51*(9), 986-997.

Sun, W., Wang, Q., Zhou, Y., & Wu, J. (2020). Material and energy flows of the iron and steel industry: Status quo, challenges and perspectives. *Applied Energy*, *268*, 114946.

Sievers, J., & Blank, T. (2023). A systematic literature review on data-driven residential and industrial energy management systems. Energies, 16(4), 1688.

Shen, F., Zhao, L., Du, W., Zhong, W., Peng, X., & Qian, F. (2022). Data-driven stochastic robust optimization for industrial energy system considering renewable energy penetration. ACS Sustainable Chemistry & Engineering, 10(11), 3690-3703.

Shahedi, A., Nasiri, M. M., Sangari, M. S., Werner, F., & Jolai, F. (2022). A stochastic multi-objective model for a sustainable closed-loop supply chain network design in the automotive industry. *Process Integration and Optimization for Sustainability*, *6*(1), 189-209.

Tehrani, M., & Gupta, S. M. (2021). Designing a sustainable green closed-loop supply chain under uncertainty and various capacity levels. *Logistics*, *5*(2), 20.

Taherifar, M., Hasani, N., Zokaee, M., Aghsami, A., & Jolai, F. (2024). A scenario-based sustainable dual-channel closed-loop supply chain design with pickup and delivery considering social conditions in a natural disaster under uncertainty: a real-life case study: M. Taherifar et al. *Environment, Development and Sustainability*, *26*(8), 19443-19490.

Ukoba, K., Yoro, K. O., Eterigho-Ikelegbe, O., Ibegbulam, C., & Jen, T. C. (2024). Adaptation of solar energy in the Global South: Prospects, challenges and opportunities. *Heliyon*, *10*(7).

Valizadeh, J., Ghahroudi, A. G., Soltani, S., Akhavan, M., Zaki, A., & Heravi, P. (2025). Mathematical modeling for the closed-loop supply chain with consideration of sustainability risks: a hybrid optimization approach. *Environment, Development and Sustainability*, *27*(5), 10593-10628.

Varne, A. R., Blouin, S., Williams, B. L. M., & Denkenberger, D. (2024). The impact of abrupt sunlight reduction scenarios on renewable energy production. *Energies*, *17*(20), 5147.

Wu, H., Ke, D., Song, L., Xu, J., Liao, S., & Wang, L. (2025). Multi-objective and multi-stage capacity planning for low-carbon iron and steel industry empowered by wind-gas-hydrogen energy. *Applied Energy*, *390*, 125793.

Watari, T., Fishman, T., Wieland, H., & Wiedenhofer, D. (2025). Global stagnation and regional variations in steel recycling. Resources, Conservation and Recycling, 220, 108363.

Wang, G., Wu, J., Yang, Y., & Su, L. (2024). Robust optimization for a steel production planning problem with uncertain demand and product substitution. *Computers & operations research*, *165*, 106569.

Wang, Z., Hölzel, H., Fernandez, L., Aslam, A. S., Baronas, P., Orrego-Hernández, J., ... & Moth-Poulsen, K. (2024). Hybrid solar energy device for simultaneous electric power generation and molecular solar thermal energy storage. *Joule*, *8*(9), 2607-2622.

Yildirim Arslan, E., & Soner Kara, S. (2026). Stochastic Multi-Objective Sustainable Supply Chain Network Design with Solar Energy and Water Footprint Integration: A Hybrid NSGA-II Approach. *Sustainability*, *18*(9), 4221.

Yavari, M., & Bohreghi, I. M. (2025). Developing a green-resilient power network and supply chain: Integrating renewable and traditional energy sources in the face of disruptions. *Applied Energy*, *377*, 124654.

Yazdi, M. Z. Z., Meyer, J. C., & Walther, G. (2026). Multi-objective supply chain optimization of renewable energy carrier imports for Europe. *Applied Energy*, *415*, 127884.

Zhou, L., Zhang, D., Li, S., & Luo, X. (2023). An integrated optimization model of green supply chain network design with inventory management. *Sustainability*, *15*(16), 12583.

Zamanipour, B., Ghadaksaz, H., Keppo, I., & Saboohi, Y. (2023). Electricity supply and demand dynamics in Iran considering climate change-induced stresses. *Energy*, *263*, 126118.

Zokaee, S., Jabbarzadeh, A., Fahimnia, B., & Sadjadi, S. J. (2017). Robust supply chain network design: an optimization model with real world application. Annals of Operations Research, 257(1), 15-44.

Zhu, J., Dong, H., Zheng, W., Li, S., Huang, Y., & Xi, L. (2022). Review and prospect of data-driven techniques for load forecasting in integrated energy systems. Applied Energy, 321, 119269.